

Hybrid Beamforming with Selection for Multi-user Massive MIMO Systems

Vishnu V. Ratnam, *Student Member, IEEE*, Andreas F. Molisch, *Fellow, IEEE*,
 Ozgun Y. Bursalioglu, *Member, IEEE*, and
 Haralabos C. Papadopoulos, *Member, IEEE*

Abstract

This work studies a variant of hybrid beamforming, namely, hybrid beamforming with selection (HBwS), as an attractive solution to reduce the hardware cost of multi-user Massive Multiple-Input-Multiple-Output systems, while retaining good performance. In a transceiver with HBwS, the antenna array is fed by an analogue beamforming matrix with L input ports. Unlike conventional hybrid beamforming, a bank of switches connects the instantaneously best K out of the L input ports to K up/down-conversion chains, where $K \leq L$. The analogue beamformer is designed based on average channel statistics and therefore needs to be updated only infrequently, while the switches operate based on instantaneous channel knowledge; this allows for a higher diversity-order, better user separability and/or simpler hardware than some conventional hybrid schemes. In this work, a novel design for the analogue beamformer is derived and approaches to reduce the hardware and computational cost of a multi-user HBwS system are explored. In addition, we study how L , the switch bank architecture, the number of data-streams, and the apriori estimated rank of the transmit spatial correlation matrix, impact system performance. Simulations suggest that HBwS enables linear coding schemes like Zero-Forcing, achieve performance comparable to Dirty Paper Coding.

Index Terms

V. V. Ratnam and A. F. Molisch are with the Ming Hsieh Department of Electrical Engineering, University of Southern California, Los Angeles, CA, 90089 USA (e-mail: {ratnam, molisch}@usc.edu)

O. Y. Bursalioglu and H. C. Papadopoulos are with Docomo Innovations, Palo Alto, CA, 94304 USA (e-mail: {obursalioglu, hpapadopoulos}@docomoinnovations.com)

Beam selection, mm-wave, Massive MIMO, Hybrid precoding with selection, Hybrid preprocessing with selection, Hybrid precoding, Hybrid preprocessing, Grassmannian manifold.

I. INTRODUCTION

Massive Multiple-input-multiple-output (MIMO) systems, enabled by using antenna arrays with many elements at the transmitter and/or receiver, are viewed as a key enabler towards meeting the rising throughput demands in cellular systems. This is due to their ability to boost spectral efficiency by increasing the spatial degrees of freedom and/or providing beamforming gains while permitting simplified transmission methods [1]. With the advances in digital and radio frequency (RF) analogue hardware technologies, and further spurred by the prospect of millimeter (mm) wave frequency bands (> 30 GHz) for data transmission, massive MIMO has also become practically viable today and is a key focus area for 5G systems [2]. It is predicted that future cellular systems will be equipped with massive antenna arrays of $100 - 1000$ antenna elements, at least at the base-station (BS) end. Although producing affordable large antenna arrays on a small footprint is already viable, the corresponding up/down-conversion chains, which include Analog-to-Digital Converters/ Digital-to-Analog Converters, filters, and mixers, are expensive and power hungry. This has motivated research on hybrid beamforming, which takes advantage of the directional nature of wireless channels [3]–[5], to feed a large antenna array to fewer up/down-conversion chains. In this work, we focus primarily on such hybrid architectures at the BS.

A. Hybrid Beamforming

In a BS with hybrid beamforming (also known as hybrid precoding/ preprocessing), an analogue RF beamforming matrix, built from analogue hardware like phase-shifters, is used to connect N antenna elements to K up/down-conversion chains, where $K \ll N$. This beamforming matrix exploits channel state information to form beams into the *dominant* angular directions of each user's channel, thereby, utilizing the transmit power more effectively and providing some multi-user separation with fewer up/down-conversion chains. Since the analogue hardware components are relatively cheap and consume less power than the up/down-converters and digital

hardware, this design leads to significant savings as compared to a full complexity transceiver, i.e., with N up/down-conversion chains. The idea was first proposed in [6]–[9] and was further investigated for the mm-wave band in [10], [11]. Since then, numerous publications have followed suit with different architectures for the analogue beamforming matrix, and 3GPP is working on including them in the upcoming 5G cellular standard [12]. An overview of the recent results is available in [13].

In one architecture called hybrid beamforming based on instantaneous channel state information (HBiCSI) [6], [14], [15], the beamforming matrix, and therefore the analogue precoding beams, adapt to the instantaneous channel state information (iCSI), as illustrated in Fig. 1a for a single user case. Though this solution promises good performance¹, iCSI across all the N transmit antennas may be required leading to a large channel estimation overhead. Additionally, it imposes strict performance specification requirements on the analogue hardware, since their parameters have to be updated in each coherence time interval, which can be very short especially for mm-wave channels. In another architecture called hybrid beamforming based on average channel state information (HBaCSI) [8], [11], [16], the beamforming matrix adapts to the average channel state information (aCSI) i.e., the transmit/receive spatial correlation matrices, as illustrated in Fig. 1b. Since aCSI changes slowly, the analogue hardware parameters need to be updated infrequently. Additionally, iCSI is only needed in the channel sub-space spanned by the analog precoding beams, leading to a significant reduction in the channel estimation overhead. Despite these benefits, the performance¹ may be worse than HBiCSI since the beams do not adapt to iCSI [16]. The performance gap may be especially large if the dimension of the dominant channel subspace² is much larger than K , which is possible both at microwave [17] and mm-wave [4] frequencies.

B. Hybrid Beamforming with Selection

Even with a small K and an aCSI based beamformer, it is possible to adapt the transmit analogue precoding beams to iCSI via the use of selection techniques [8]. By using additional

¹By system performance we refer to the capacity/throughput excluding the channel estimation overhead.

²It represents the channel subspace at the transmitter along which most of the channel power is concentrated. Such a notion is quite common for massive MIMO and is used in several proposed schemes like Joint Space Division Multiplexing [16].

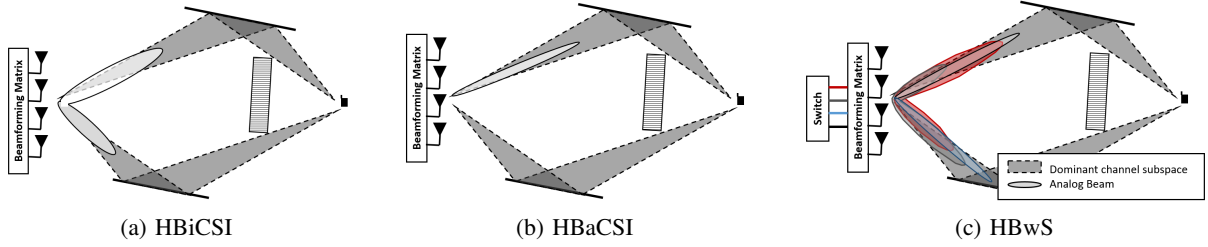


Fig. 1. An illustration of the different hybrid beamforming schemes at a transmitter with one up-conversion chain, given dominant angular directions and a single antenna receiver.

analogue hardware, several possible options for the analog precoding beams can be provided, as illustrated in Fig. 1c. By dynamically switching to the “best” beams for each channel realization, we may obtain performance¹ comparable to HBiCSI.

In this paper we study a generalization of this approach, namely, hybrid beamforming with selection (HBwS), as a solution to achieve performance¹ comparable to HBiCSI, while still retaining some benefits of HBaCSI i.e., infrequent update of analogue hardware parameters and low channel estimation overhead. The block diagram of a transmitter (TX) with HBwS is given in Fig. 2a. Here, we again have an analogue beamforming matrix that is connected to the antennas. However, unlike conventional hybrid beamforming, the number of input ports for the beamforming matrix (L) is larger than the number of available up-conversion chains (K). This matrix is preceded by a bank of K one-to-many RF switches, each of which can connect one up-conversion chain to one of several input ports. Note that each connection of the K up-conversion chains to K out-of-the L input ports corresponds to a distinct analog precoding beam in Fig. 1c. While the beamforming matrix is designed based on aCSI, the switches exploit iCSI to optimize this K out-of-the L input port selection. The premise for this design is that unlike phase shifters, RF switches are cheap and can be easily designed to switch quickly based on iCSI [8], [18]. Since $L > K$ and switches adapt the *effective* precoding beams to iCSI, a higher diversity-order and a larger beamforming gain can be achieved in comparison to HBaCSI. Furthermore, due to its superior beam-shaping capabilities, HBwS provides better user separation than HBaCSI in a multi-user system.

On the downside, the channel estimation overhead for HBwS may be larger than for HBaCSI.

An analysis of the channel estimation overhead is beyond the scope of this paper, see [18], [19] for some preliminary results. Similarly, since the beamformer has a size of $N \times L$, as opposed to $N \times K$ for HBaCSI, a larger number of analogue components are required for HBwS. Techniques to reduce the number of these components are discussed later in section VII.

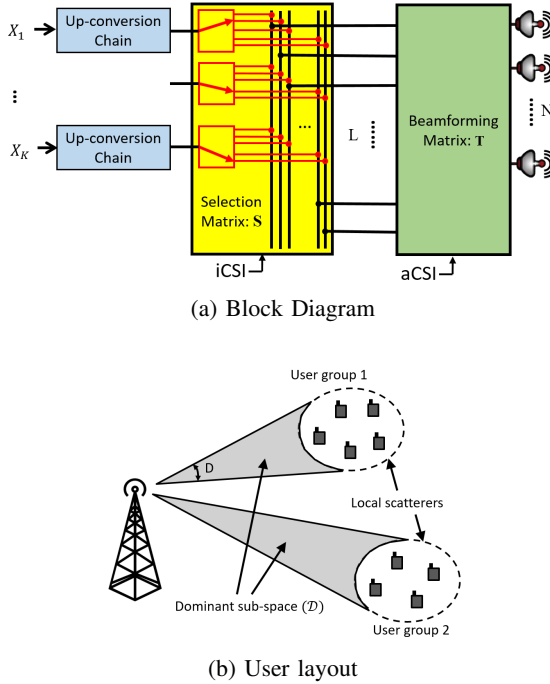


Fig. 2. Illustration of: (a) a Block diagram of Hybrid Beamforming with Selection at the TX (b) a sample user layout

The simplest case of HBwS is antenna selection [20]–[22], where the analogue beamforming matrix is omitted. Soon it was shown that introducing a beamforming stage provides additional beamforming gain, and several designs for the beamforming matrix have been proposed [7], [8]. More recently, antenna selection has also been explored with regard to cost, power consumption and channel estimation overhead [18]. However in most of the prior work, the beamforming matrix is unitary, where the number of input ports (L) equals the number of transmit antennas (N), i.e., it spans the whole channel dimension. Though some of these designs [7], [8], can be extended to the case of $L < N$ (but not $L > N$), these designs are inferior, especially in spatially sparse channels [23]. A generic design for the beamforming matrix in a single user multiple-input-single-output scenario was proposed by us in [23] and shown to provide improved performance. This work extends this design to a multi-user MIMO scenario while also taking

into account the impact of the switch bank architecture. Further, we investigate the hardware implementation cost of HBwS. The contributions of this paper are as follows:

- 1) We propose a generic architecture of HBwS for low complexity multi-user MIMO transceivers, wherein the beamforming matrix may be a non-unitary rectangular matrix i.e., $L \neq N$.
- 2) For a channel with isotropic scattering within the dominant channel subspace², we show that a beamforming matrix that maximizes a lower bound to the system sum capacity can be obtained via a coupled Grassmannian subspace packing problem.
- 3) We find a good sub-optimal solution to this packing problem and propose algorithms to improve it.
- 4) We propose a two-stage architecture for the beamformer and find a family of “good” switch positions, which help reduce the computational and hardware cost of HBwS while retaining good performance.
- 5) An extension of the beamformer design to channels with anisotropic scattering is also explored.

The organization of this paper is as follows: the general assumptions and the channel model are discussed in Section II; the expression for the system capacity and the beamforming matrix design problem are formulated in Section III; the search-space for the optimal beamformer is characterized in Section IV and a closed-form lower bound to the objective function is explored in Section V; a good beamformer design and algorithms for further improving upon it are discussed in Section VI; strategies to reduce the hardware implementation cost for HBwS are discussed in Section VII; the simulation results are presented in Section VIII; the extension to anisotropic channels is considered in Section IX; and finally, the conclusions are summarized in Section X.

Notation used in this work is as follows: scalars are represented by light-case letters; vectors by bold-case letters; matrices are represented by capitalized bold-case letters and sets and subspaces are represented by calligraphic letters. Additionally, \mathbf{a}_i represents the i -th element of a vector \mathbf{a} , $|\mathbf{a}|$ represents the L_2 norm of a vector \mathbf{a} , $\mathbf{A}_{i,j}$ represents the (i, j) -th element of a matrix \mathbf{A} , $[\mathbf{A}]_{c\{i\}}$ and $[\mathbf{A}]_{r\{i\}}$ represent the i -th column and row vectors of matrix \mathbf{A} respectively, $\|\mathbf{A}\|_F$ represents the Frobenius norm of a matrix \mathbf{A} , \mathbf{A}^\dagger is the conjugate transpose of a matrix \mathbf{A} and $|\mathcal{A}|$ represents the cardinality of a set \mathcal{A} or dimension of a space \mathcal{A} . Also, ${}^N C_k = \frac{N!}{(N-k)!k!}$

where $N!$ is the factorial of N , $\stackrel{d}{=}$ is equivalence in distribution, $\mathbb{E}\{\cdot\}$ represents the expectation operator, \mathbb{P} is the probability operator, \mathbb{I}_i and $\mathbb{O}_{i,j}$ are the $i \times i$ and $i \times j$ identity and zero matrices respectively, and \mathbb{R} and \mathbb{C} represent the field of real and complex numbers.

II. GENERAL ASSUMPTIONS AND CHANNEL MODEL

We consider a downlink multi-user massive MIMO broadcast channel where the BS has $N \gg 1$ antennas but only $K \leq N$ up-conversion chains, and implements HBwS.³ The TX RF analogue beamforming matrix has a dimension of $N \times L$ and a bank of switches, denoted by a selection matrix \mathbf{S} , is used to connect K out-of-the L input ports of the beamforming matrix with the up-conversion chains. The system has M_1 receivers, i.e., each having M_2 antennas and M_2 down-conversion chains, where $K \geq M_1 M_2$. We assume a narrow-band system with a frequency flat and temporally block fading channel. Under these assumptions, the baseband equivalent downlink received signal at user m , for a given selection matrix \mathbf{S} , can be expressed as:

$$\mathbf{y}_m(\mathbf{S}) = \sqrt{\rho} \tilde{\mathbf{H}}_m \mathbf{T} \mathbf{S} \underbrace{\mathbf{G} \mathbf{u}}_{\mathbf{x}} + \mathbf{n}_m \quad (1)$$

where $\mathbf{y}_m(\mathbf{S})$ is the $M_2 \times 1$ received signal vector at user m , ρ is the mean receive signal-to-noise ratio (SNR), $\tilde{\mathbf{H}}_m$ is the $M_2 \times N$ downlink channel matrix for user m , \mathbf{T} is the $N \times L$ beamforming matrix composed of analogue hardware, \mathbf{S} is a $L \times K$ sub-matrix of the identity matrix \mathbb{I}_L - formed by picking K out-of-the L columns, $\mathbf{x} \triangleq \mathbf{G} \mathbf{u}$ is the $K \times 1$ transmit data vector from the up-conversion chains and $\mathbf{n}_m \sim \mathcal{CN}(\mathbb{O}_{M_2 \times M_2}, \mathbb{I}_{M_2})$ is the normalized additive white Gaussian noise observed at user m . Here \mathbf{G} is a $K \times K$ a full-rank matrix that ortho-normalizes the columns of $\mathbf{T} \mathbf{S}$ i.e., $\mathbf{G}^\dagger \mathbf{S}^\dagger \mathbf{T}^\dagger \mathbf{T} \mathbf{S} \mathbf{G} = \mathbb{I}_K$. Here we implicitly assume that $\mathbf{T} \mathbf{S}$ has linearly independent columns for each \mathbf{S} . The transmit power constraint can then be expressed as:

$$\text{tr}\{\mathbf{T} \mathbf{S} \mathbb{E}_{\mathbf{x}}\{\mathbf{x} \mathbf{x}^\dagger\} \mathbf{S}^\dagger \mathbf{T}^\dagger\} \leq 1 \quad (2a)$$

$$\Rightarrow \mathbb{E}_{\mathbf{u}}\{\mathbf{u} \mathbf{u}^\dagger\} \leq 1. \quad (2b)$$

³The presented results can also be extended to an uplink MAC channel with HBwS at the BS.

We assume that the instantaneous channel realizations (or iCSI) $\{\tilde{\mathbf{H}}_1, \dots, \tilde{\mathbf{H}}_{M_1}\}$ are known at the TX and contain both a large scale fading as well as a small scale fading component. The small scale fading statistics are assumed to be Rayleigh in amplitude and doubly spatially correlated (both at transmitter and receiver end). We focus on the scenario assumptions considered in [16], wherein the users can be divided into user groups with common intra-group channel statistics and orthogonal channels across the groups, as illustrated in Fig. 2b. Since such orthogonal user groups can be treated separately, without loss of generality, we assume these M_1 receivers belong to one group. As illustrated in Fig. 2b, such users are close enough to share the same set of local scatterers, but are sufficient wavelengths apart to undergo independent and identically distributed (i.i.d.) small scale fading. Therefore, we assume that the channels to the different users are independently distributed and follow the widely used Kronecker correlation model [24] with a common transmit spatial correlation matrix \mathbf{R}_{tx} but individual receive correlation matrices $\mathbf{R}_{rx,m}$, respectively [16]. To model a, possibly, spatially sparse channel [3]–[5], we assume \mathbf{R}_{tx} has rank D , where $K < D \leq N$. Under these conditions, the channel matrices can be expressed as:

$$\tilde{\mathbf{H}}_m = \mathbf{R}_{rx,m}^{1/2} \mathbf{H}_m [\Lambda_{tx}^D]^{1/2} [\mathbf{E}_{tx}^D]^\dagger \quad (3)$$

where \mathbf{H}_m is an $M_2 \times D$ matrix with i.i.d. $\mathcal{CN}(0, 1)$ entries and $\Lambda_{tx}^D, \mathbf{E}_{tx}^D$ are the $D \times D, N \times D$ matrices of eigenvalues and eigen-vectors of \mathbf{R}_{tx} , respectively, corresponding to the D non-zero eigenvalues. We shall refer to $\mathcal{D} \triangleq \text{column-space}\{\mathbf{E}_{tx}^D\}$: the channel sub-space at TX containing all the power to the M_1 same-group users, as the *dominant channel subspace* (see Fig. 2b). Without loss of generality, the mean pathloss for the user group is included into ρ and any user specific large scale fading components are included in $\mathbf{R}_{rx,m}$.

The beamforming matrix is updated based on knowledge of only the spatial correlation matrices $\mathbf{R}_{tx}, \mathbf{R}_{rx,m}$ but the selection matrix \mathbf{S} is updated based on iCSI. For ease of analysis, we shall first consider the case of $\Lambda_{tx}^D = \frac{N}{D} \mathbb{I}_D$ in Section V. Such isotropic scattering in \mathcal{D} is reasonable when there are sufficiently large number of local scatterers. We also extend the results to the more general case of $\Lambda_{tx}^D \neq \frac{N}{D} \mathbb{I}_D$ in Section IX.

III. PROBLEM FORMULATION

Let $\mathcal{S} \triangleq \{\mathbf{S}_1, \dots, \mathbf{S}_{|\mathcal{S}|}\}$ denote the set of all feasible selection matrices. Note that depending on the switch bank architecture, this set, referred to as the switch position set, may not involve all the $\binom{L}{K}$ choices. For each $\mathbf{S}_i \in \mathcal{S}$, let \mathbf{G}_i be the corresponding orthogonalization matrix in (1) i.e., $\mathbf{G}_i^\dagger \mathbf{S}_i^\dagger \mathbf{T}^\dagger \mathbf{T} \mathbf{S}_i \mathbf{G}_i = \mathbb{I}_K$. Although \mathbf{G}_i is also a function of \mathbf{T} , this dependence is not explicitly shown for ease of representation. For a given selection matrix \mathbf{S}_i , note that the down-link channel described in section II is a broadcast channel with effective channel matrices $\tilde{\mathbf{H}}_m \mathbf{T} \mathbf{S}_i \mathbf{G}_i$ for each user m . Therefore, using uplink-downlink duality [25] and results in [26], a lower bound to the achievable ergodic sum rate of the system in (1) can be expressed as:

$$\begin{aligned} C(\mathbf{T}) &\triangleq \mathbb{E}_{\tilde{\mathbf{H}}} \left\{ \max_{1 \leq i \leq |\mathcal{S}|} \log \left| \mathbb{I}_N + \sum_{m=1}^{M_1} \frac{\rho}{M} \mathbf{G}_i^\dagger \mathbf{S}_i^\dagger \mathbf{T}^\dagger \tilde{\mathbf{H}}_m^\dagger \tilde{\mathbf{H}}_m \mathbf{T} \mathbf{S}_i \mathbf{G}_i \right| \right\} \\ &= \mathbb{E}_{\tilde{\mathbf{H}}} \left\{ \max_{1 \leq i \leq |\mathcal{S}|} \log \left| \mathbb{I}_M + \frac{\rho}{M} \tilde{\mathbf{H}} \mathbf{T} \mathbf{S}_i \mathbf{G}_i \mathbf{G}_i^\dagger \mathbf{S}_i^\dagger \mathbf{T}^\dagger \tilde{\mathbf{H}}^\dagger \right| \right\} \end{aligned} \quad (4)$$

where we define $\tilde{\mathbf{H}}^\dagger = \begin{bmatrix} \tilde{\mathbf{H}}_1^\dagger & \tilde{\mathbf{H}}_2^\dagger & \dots & \tilde{\mathbf{H}}_{M_1}^\dagger \end{bmatrix}$ and $M \triangleq M_1 M_2$. This lower bound is asymptotically tight for a large signal-to-noise ratio (SNR) [26]. Furthermore, from (3) and the fact that $\tilde{\mathbf{H}}_m$ are independent for all m , we can express:

$$\tilde{\mathbf{H}} = \mathbf{R}_{\text{rx}}^{1/2} \mathbf{H} [\Lambda_{\text{tx}}^D]^{1/2} [\mathbf{E}_{\text{tx}}^D]^\dagger \quad (5)$$

where \mathbf{R}_{rx} is a block-diagonal matrix with the m -th diagonal block being $\mathbf{R}_{\text{rx},m}$ and $\mathbf{H} = \begin{bmatrix} \mathbf{H}_1^\dagger & \mathbf{H}_2^\dagger & \dots & \mathbf{H}_{M_1}^\dagger \end{bmatrix}^\dagger$ is a $M \times D$ matrix with i.i.d. $\mathcal{CN}(0, 1)$ entries. The primary goal of this work is to find the analogue beamformer \mathbf{T} that maximizes the lower bound in (4), i.e.,:

$$\mathbf{T}_{\text{opt}} = \text{argmax}_{\mathbf{T} \in \mathbb{C}^{N \times L}} \{C(\mathbf{T})\} \quad (6)$$

where \mathbf{T}_{opt} is designed based on the knowledge of the aCSI statistics: \mathbf{R}_{tx} and \mathbf{R}_{rx} . Here, with slight abuse of notation, by $\text{argmax}\{\}$ we refer to any one of the (possibly many) maximizing arguments. As shall be seen later, an exact solution to (6) is intractable and we shall therefore restrict ourselves to a good sub-optimal solution, that only requires knowledge of \mathbf{R}_{tx} .

A. Connections to limited-feedback precoding

Note that HBwS is an example of a restricted precoded system [27]. In fact, by considering the precoding matrices for the different switch positions $\{\mathbf{T}\mathbf{S}_i\mathbf{G}_i|\mathbf{S}_i \in \mathcal{S}\}$ as entries of a codebook, the single user case ($M_1 = 1$) can be interpreted as a type of limited-feedback unitary precoding [28], [29]. However, in contrast to conventional limited-feedback precoding, the HBwS codebook entries $\{\mathbf{T}\mathbf{S}_i\mathbf{G}_i|\mathbf{S}_i \in \mathcal{S}\}$ are coupled, as they are generated from the columns of the same beamforming matrix \mathbf{T} . As a result, good codebook designs for limited-feedback unitary precoding [30]–[32] cannot be directly extended to find good designs for \mathbf{T} .

IV. RESTRICTING THE SEARCH SPACE

Notice that in (6), search for \mathbf{T}_{opt} is over all possible $N \times L$ complex matrices. In this Section, we reduce the dimension of the search space by getting rid of some sub-optimal and redundant solutions.

Theorem IV.1 (Restricting to dominant sub-space). *There exists an optimal solution \mathbf{T}_{opt} to (6) such that, $\mathbf{T}_{\text{opt}} = \mathbf{E}_{\text{tx}}^D \hat{\mathbf{T}}_{\text{opt}}$, where $\hat{\mathbf{T}}_{\text{opt}}$ is a solution to:*

$$\hat{\mathbf{T}}_{\text{opt}} = \underset{\hat{\mathbf{T}} \in \mathbb{C}^{D \times L}}{\text{argmax}} \left\{ C^D(\hat{\mathbf{T}}) \right\} \quad (7)$$

$$C^D(\hat{\mathbf{T}}) \triangleq \mathbb{E}_{\mathbf{H}} \left\{ \max_{1 \leq i \leq |\mathcal{S}|} \log \left| \mathbb{I}_M + \frac{\rho}{M} \mathbf{R}_{\text{rx}}^{1/2} \mathbf{H} [\Lambda_{\text{tx}}^D]^{1/2} \hat{\mathbf{T}} \mathbf{S}_i \hat{\mathbf{G}}_i \hat{\mathbf{G}}_i^\dagger \mathbf{S}_i^\dagger \hat{\mathbf{T}}^\dagger [\Lambda_{\text{tx}}^D]^{1/2} \mathbf{H}^\dagger \mathbf{R}_{\text{rx}}^{1/2} \right| \right\}, \quad (8)$$

\mathbf{H} is as defined in (5) and $\hat{\mathbf{G}}_i$ ortho-normalizes columns of $\hat{\mathbf{T}} \mathbf{S}_i$.

Proof. See Appendix A. □

Intuitively, this theorem states that since all the channel power is concentrated in the dominant channel subspace \mathcal{D} , the beams created by \mathbf{T} for any switch position should point into \mathcal{D} . Henceforth we shall restrict to finding the optimal solution $\hat{\mathbf{T}}_{\text{opt}}$ to (7), since \mathbf{T}_{opt} can be found in a straightforward way from it. In fact, as shall be shown later in Section VII-A, expressing \mathbf{T}_{opt} as $\mathbf{E}_{\text{tx}}^D \hat{\mathbf{T}}_{\text{opt}}$ may also help reduce the hardware cost for implementing the analogue beamforming matrix. To prevent any confusion, we shall henceforth refer to $\hat{\mathbf{T}}_{\text{opt}}$ as the reduced dimensional

(RD) beamformer. Though (7) reduces the search space from $\mathbb{C}^{N \times L}$ to $\mathbb{C}^{D \times L}$, it is still unbounded. This problem is remedied by the following theorem.

Theorem IV.2 (Bounding the search space). *For any $\hat{\mathbf{T}} \in \mathbb{C}^{D \times L}$, both $\hat{\mathbf{T}}$ and $\hat{\mathbf{T}}\Lambda_\theta$ attain the same sum capacity (8), where Λ_θ is any arbitrary $L \times L$ complex diagonal matrix.*

Proof. See Appendix B. □

From theorem IV.2, by replacing $\hat{\mathbf{T}}$ by $\hat{\mathbf{T}}_\theta = \hat{\mathbf{T}}\Lambda_\theta$ in (7), where:

$$[\Lambda_\theta]_{\ell,\ell} = \frac{[\hat{\mathbf{T}}_{1,\ell}]^\dagger}{|[\hat{\mathbf{T}}]_{c\{\ell\}}| |\hat{\mathbf{T}}_{1,\ell}|} \quad \forall 1 \leq \ell \leq L$$

the optimal RD-beamformer design problem can be reduced to:

$$\begin{aligned} \hat{\mathbf{T}}_{\text{opt}} &= \underset{\hat{\mathbf{T}} \in \mathcal{T}_G}{\text{argmax}} \left\{ C^D(\hat{\mathbf{T}}) \right\} \quad \text{where,} \\ \mathcal{T}_G &= \left\{ \hat{\mathbf{T}} \in \mathbb{C}^{D \times L} \left| |[\hat{\mathbf{T}}]_{c\{\ell\}}| = 1, \text{Im}\{\hat{\mathbf{T}}_{\ell,1}\} = 0 \quad \forall \ell = 1, \dots, L \right. \right\} \end{aligned} \quad (9)$$

where, $\text{Im}\{\}$ represents the imaginary component. Note that since the ergodic sum capacity $C^D(\hat{\mathbf{T}})$ is invariant to complex scaling of the columns of $\hat{\mathbf{T}}$, each column $[\hat{\mathbf{T}}]_{c\{\ell\}}$ for $1 \leq \ell \leq L$ is representative of a 1-dimensional linear subspace in $\mathbb{C}^{D \times 1}$. Therefore, (9) is actually an optimization problem over the complex Grassmannian manifold $\mathcal{G}(D, 1)$ ⁴.

V. LOWER BOUND ON THE OBJECTIVE FUNCTION

Though restrictions on search space were introduced in the previous section to reduce the search complexity, the ergodic sum capacity $C^D(\hat{\mathbf{T}})$ is not in closed form. A closed-form lower bound to $C^D(\hat{\mathbf{T}})$ for the case of $M = 1$ was considered in [23] which was shown to be maximized by Grassmannian line-packing the columns of $\hat{\mathbf{T}}$. However, this bound is independent of the switch position set \mathcal{S} and cannot be generalized to $M > 1$. Similarly, another approximation to $C^D(\hat{\mathbf{T}})$ can be obtained via the work on restricted precoding [27]. Though this approximation eliminates the need for taking an expectation as in (8), it has to be computed recursively and

⁴The complex Grassmannian manifold $\mathcal{G}(A, B)$ is defined as the set of all B dimensional linear sub-spaces of a vector space of dimension A , with field \mathbb{C} .

is accurate only when $D, K \gg M$. In contrast, the metric we present in this section provides a closed-form lower bound to the sum capacity that depends on \mathcal{S} . Henceforth, for ease of analysis, we assume $\Lambda_{\text{tx}}^D = \frac{N}{D} \mathbb{I}_D$. Extension to more generic channels is considered later in section IX.

For any $a > b > 0$, we define the complex Stiefel manifold $\mathcal{U}(a, b)$ as the set of all $a \times b$ matrices with ortho-normal columns. We shall refer to such matrices as semi-unitary matrices. For ease of notation, we further define $\mathbf{Q}_i \triangleq \hat{\mathbf{T}} \mathbf{S}_i \hat{\mathbf{G}}_i$ for each selection matrix $\mathbf{S}_i \in \mathcal{S}$. Note that $\mathbf{Q}_i \in \mathcal{U}(D, K)$ for all $i = 1, \dots, |\mathcal{S}|$. We also define the Fubini-Study distance between two matrices $\mathbf{A}, \mathbf{B} \in \mathcal{U}(D, K)$ as:

$$d_{\text{FS}}(\mathbf{A}, \mathbf{B}) = \arccos \sqrt{|\mathbf{A}^\dagger \mathbf{B} \mathbf{B}^\dagger \mathbf{A}|} \quad (10)$$

It quantifies the distance between the column-spaces of \mathbf{A} and \mathbf{B} over the Grassmannian manifold $\mathcal{G}(D, K)$. We then have the following lemma:

Lemma V.1 (Higher dimension lower bound). *If $\Lambda_{\text{tx}}^D = \frac{N}{D} \mathbb{I}_D$, we have $C^{\mathcal{D}}(\hat{\mathbf{T}}) \geq C_{\text{LB1}}^{\mathcal{D}}(\hat{\mathbf{T}})$ where:*

$$C_{\text{LB1}}^{\mathcal{D}}(\hat{\mathbf{T}}) \triangleq \mathbb{E}_{\mathbf{H}} \mathbb{E}_{\mathbf{V}} \left\{ \max_{1 \leq i \leq |\mathcal{S}|} \log \left[1 + \alpha \left| \mathbf{V}^\dagger \mathbf{Q}_i \mathbf{Q}_i^\dagger \mathbf{V} \right| \right] \right\}, \quad (11)$$

$\alpha = \left(\frac{\rho N}{MD} \right)^M |\mathbf{R}_{\text{rx}}| |\mathbf{H} \mathbf{H}^\dagger|$, \mathbf{H} is as defined in (5) and \mathbf{V} is a random matrix uniformly distributed over $\mathcal{U}(D, K)$, independent of \mathbf{H} .

Proof. See appendix C □

Note that in (8), each \mathbf{Q}_i is associated with a corresponding selection region: $\{\mathbf{H} \in \mathbb{C}^{M \times D} | i = \text{argmax}_{1 \leq j \leq |\mathcal{S}|} |\mathbb{I}_M + \frac{\rho N}{MD} \mathbf{R}_{\text{rx}}^{1/2} \mathbf{H} \mathbf{Q}_j \mathbf{Q}_j^\dagger \mathbf{H}^\dagger \mathbf{R}_{\text{rx}}^{1/2}| \}$. Essentially, lemma V.1 finds a lower bound where these selection regions are changed to $\{\mathbf{V} \in \mathcal{U}(D, K) | i = \text{argmax}_{1 \leq j \leq |\mathcal{S}|} |\mathbf{V}^\dagger \mathbf{Q}_j \mathbf{Q}_j^\dagger \mathbf{V}| \}$. These regions are easier to bound than those in (8), as exploited by the following theorem.

Theorem V.1 (Fubini-Study lower bound). *If $\Lambda_{\text{tx}}^D = \frac{N}{D} \mathbb{I}_D$ and $D \gg 1$, we have $C^{\mathcal{D}}(\hat{\mathbf{T}}) \geq C_{\text{LB}}^{\mathcal{D}}(\hat{\mathbf{T}})$, where:*

$$C_{\text{LB}}^{\mathcal{D}}(\hat{\mathbf{T}}) \triangleq |\mathcal{S}| \left(\frac{1 - \cos^{2/K}(\delta/2)}{K} \right)^{DK+\epsilon} [\beta + \log \cos^2(\delta/2)], \quad (12a)$$

$$\delta = \min_{i \neq j} \left\{ \frac{d_{\text{FS}}(\mathbf{Q}_i, \mathbf{Q}_j)}{\sqrt{K}} \right\}, \quad (12\text{b})$$

$$\beta = M \log \left(\frac{\rho N}{MD} \right) + \log |\mathbf{R}_{\text{rx}}| + \sum_{m=1}^M \psi(D - m + 1), \quad (12\text{c})$$

$\psi()$ being the digamma function and $\epsilon = o(D)$ i.e., $\lim_{D \rightarrow \infty} \epsilon/D = 0$. Furthermore, if $\beta \geq 2$:

$$\text{argmax}_{\hat{\mathbf{T}} \in \mathcal{T}_{\mathcal{G}}} \left\{ C_{\text{LB}}^{\mathcal{D}}(\hat{\mathbf{T}}) \right\} \equiv \text{argmax}_{\hat{\mathbf{T}} \in \mathcal{T}_{\mathcal{G}}} \left\{ f_{\text{FS}}(\hat{\mathbf{T}}) \right\} \quad (13)$$

where, $f_{\text{FS}}(\hat{\mathbf{T}}) = \min_{i \neq j} d_{\text{FS}}(\mathbf{Q}_i, \mathbf{Q}_j)$.

Proof. Consider \mathbf{V} uniformly distributed over $\mathcal{U}(D, K)$ as in Lemma V.1. Since both \mathbf{V} and \mathbf{Q}_i are semi-unitary, we have $0 \leq |\mathbf{V}^\dagger \mathbf{Q}_i \mathbf{Q}_i^\dagger \mathbf{V}| \leq 1$. Let us define $\delta \triangleq \min_{i \neq j} d_{\text{FS}}(\mathbf{Q}_i, \mathbf{Q}_j)$ for $1 \leq i, j \leq |\mathcal{S}|$. Then the regions:

$$\begin{aligned} \mathcal{V}_i &= \left\{ \mathbf{V} \mid d_{\text{FS}}(\mathbf{V}, \mathbf{Q}_i) < \delta/2 \right\} \\ &= \left\{ \mathbf{V} \mid |\mathbf{V}^\dagger \mathbf{Q}_i \mathbf{Q}_i^\dagger \mathbf{V}| > \cos^2(\delta/2) \right\} \end{aligned}$$

are all disjoint [33]. Therefore, by pessimistically assuming that $|\mathbf{V}^\dagger \mathbf{Q}_i \mathbf{Q}_i^\dagger \mathbf{V}| = 0$ when $\mathbf{V} \notin \bigcup_i \mathcal{V}_i$ and $|\mathbf{V}^\dagger \mathbf{Q}_i \mathbf{Q}_i^\dagger \mathbf{V}| = \cos(\delta/2)$ when $\mathbf{V} \in \bigcup_i \mathcal{V}_i$, we can lower bound $C_{\text{LB1}}^{\mathcal{D}}(\hat{\mathbf{T}})$ in (11) as:

$$\begin{aligned} C_{\text{LB1}}^{\mathcal{D}}(\hat{\mathbf{T}}) &\geq \mathbb{P}\left(\mathbf{V} \in \bigcup_i \mathcal{V}_i\right) \mathbb{E}_{\mathbf{H}} \log[\alpha \cos^2(\delta/2)] \\ &= \sum_{i=1}^{|\mathcal{S}|} \mathbb{P}(\mathbf{V} \in \mathcal{V}_i) [\beta + \log \cos^2(\delta/2)] \end{aligned} \quad (14)$$

where β is given by (12c) and follows from the results on log-determinant of a Wishart matrix [34].⁵ Since \mathbf{V} is uniformly distributed over $\mathcal{U}(D, K)$, based on results in [28], [35], we have:

$$\sum_{i=1}^{|\mathcal{S}|} \mathbb{P}(\mathbf{V} \in \mathcal{V}_i) \geq |\mathcal{S}| \left(\frac{1 - \cos^{2/K}(\delta/2)}{K} \right)^{DK+\epsilon} \quad (15)$$

where $\epsilon = o(D)$. Using (14)–(15) and lemma V.1, we arrive at (12a).

Note that $\hat{\mathbf{T}}$ affects $C_{\text{LB}}^{\mathcal{D}}(\hat{\mathbf{T}})$ only via the term δ (for a fixed L). Therefore, if the partial

⁵Note that $|\mathbf{H}\mathbf{H}^\dagger|$ is the determinant of a $M \times M$ complex Wishart matrix with D degrees of freedom.

derivative of $C_{\text{LB}}^{\mathcal{D}}(\hat{\mathbf{T}})$ with respect to δ is non-negative, then maximizing δ is equivalent to maximizing $C_{\text{LB}}^{\mathcal{D}}(\hat{\mathbf{T}})$. The required condition can be found as $\frac{\partial C_{\text{LB}}^{\mathcal{D}}(\hat{\mathbf{T}})}{\partial \cos^2(\delta/2)} \leq 0$ i.e.,

$$(DK + \epsilon) \frac{\cos^{2/K}(\delta/2)}{K} [\beta + \log \cos^2(\delta/2)] \geq 1 - \cos^{2/K}(\delta/2) \quad (16)$$

Since $\cos(\delta) = \min_{i \neq j} \sqrt{|\mathbf{Q}_i^\dagger \mathbf{Q}_j \mathbf{Q}_j^\dagger \mathbf{Q}_i|} \geq 0$, we have $\cos^2(\delta/2) = \frac{\cos(\delta)+1}{2} \geq \frac{1}{2}$. Therefore a sufficient condition for (16) can be obtained as:

$$(D + \frac{\epsilon}{K}) [\beta - \log 2] \geq 2^{1/K} - 1$$

Assuming $|\epsilon| \leq KD/2$ for $D \gg 1$, it can be verified that the above holds for $\beta \geq 2$. \square

Since the objective in (9) seems intractable, for $\Lambda_{\text{tx}}^D = \frac{N}{D} \mathbb{I}_D$, we consider the sub-optimal RD-beamformer design problem that maximizes $f_{\text{FS}}(\hat{\mathbf{T}})$ in (13), i.e., we focus on finding:

$$\hat{\mathbf{T}}_{\text{FS}} = \operatorname{argmax}_{\hat{\mathbf{T}} \in \mathcal{T}_g} \left\{ f_{\text{FS}}(\hat{\mathbf{T}}) \right\} \quad (17)$$

While it only maximizes a lower bound $C_{\text{LB}}^{\mathcal{D}}(\hat{\mathbf{T}})$ to the capacity, the metric $f_{\text{FS}}(\hat{\mathbf{T}})$ can be readily computed for each candidate $\hat{\mathbf{T}}$ unlike $C^{\mathcal{D}}(\hat{\mathbf{T}})$ in (8).

A. Alternate interpretation of the Fubini-Sudy distance metric - $f_{\text{FS}}(\hat{\mathbf{T}})$

Note that for $\Lambda_{\text{tx}}^D = \frac{N}{D} \mathbb{I}_D$, the sum capacity of the RD-beamformer in (8) can be expressed as:

$$C^{\mathcal{D}}(\hat{\mathbf{T}}) = \mathbb{E}_{\mathbf{H}} \max_{1 \leq i \leq |\mathcal{S}|} \left\{ C_i^{\mathcal{D}}(\hat{\mathbf{T}}, \mathbf{H}) \right\} \quad (18)$$

where, $C_i^{\mathcal{D}}(\hat{\mathbf{T}}, \mathbf{H}) = \log \left| \mathbb{I}_M + \frac{\rho N}{MD} \mathbf{R}_{\text{rx}}^{1/2} \mathbf{H} \mathbf{Q}_i \mathbf{Q}_i^\dagger \mathbf{H}^\dagger \mathbf{R}_{\text{rx}}^{1/2} \right|$. Based on the results on restricted pre-coding [27], these individual capacities $C_i^{\mathcal{D}}(\hat{\mathbf{T}}, \mathbf{H})$ are approximately jointly Gaussian distributed with second order statistics given by:

$$\mathbb{E}\{C_i^{\mathcal{D}}(\hat{\mathbf{T}}, \mathbf{H})\} \approx M \log \left(\frac{\rho N K^{3/2}}{MD \sqrt{K+1}} \right) + \log |\mathbf{R}_{\text{rx}}| \quad (19a)$$

$$\text{Crosscov} \left\{ C_i^{\mathcal{D}}(\hat{\mathbf{T}}, \mathbf{H}), C_j^{\mathcal{D}}(\hat{\mathbf{T}}, \mathbf{H}) \right\} \approx M \log \left[1 + \frac{\|\mathbf{Q}_j^\dagger \mathbf{Q}_i\|_F^2}{K^2} \right]$$

$$\geq M \log \left[1 + \frac{\cos(d_{\text{FS}}(\mathbf{Q}_i, \mathbf{Q}_j))^{2/K}}{K} \right] \quad (19b)$$

where the last step follows by applying the AM-GM inequality on eigenvalues of $\mathbf{Q}_j^\dagger \mathbf{Q}_i \mathbf{Q}_i^\dagger \mathbf{Q}_j$ and using (10). Therefore, by maximizing $f_{\text{FS}}(\hat{\mathbf{T}})$, we minimize a lower bound to the largest cross-covariance term among the individual capacities $\{C_i^{\mathcal{D}}(\hat{\mathbf{T}}, \mathbf{H})\}$.⁶ This is an intuitively pleasing result, since reducing cross-covariance typically shifts the probability distribution of the maximum of a set of Gaussian random variables to the right [36].

VI. DESIGN OF THE BEAMFORMING MATRIX

As also mentioned in Section III-A, the design of $\hat{\mathbf{T}}_{\text{FS}}$ in (17) is different from the problem of Grassmannian subspace packing, for which several efficient algorithms are available in literature (see [37] and references therein). The difference stems from the fact that $\mathbf{Q}_i = \hat{\mathbf{T}} \mathbf{S}_i \hat{\mathbf{G}}_i$ for $i = \{1, \dots, |\mathcal{S}|\}$ are generated from the same RD-beamformer $\hat{\mathbf{T}}$. They are therefore coupled, making (17) a *coupled* Grassmannian sub-space packing problem. No known solutions are available to this problem for the best of our knowledge. However, a related problem is the problem of Grassmannian line-packing:

$$\hat{\mathbf{T}}_{\text{LP}} = \text{argmax}_{\hat{\mathbf{T}} \in \mathcal{T}_{\mathcal{G}}} \min_{i \neq j} \left\{ d_{\text{FS}}([\hat{\mathbf{T}}]_{c\{i\}}, [\hat{\mathbf{T}}]_{c\{j\}}) \right\} \quad (20)$$

for which several near-optimal solutions are available in literature [37], [38]. For $L \leq D$, both $\hat{\mathbf{T}}_{\text{FS}}$ and $\hat{\mathbf{T}}_{\text{LP}}$ are equivalent, given by any $D \times L$ semi-unitary matrix⁷. While this is not true for $L > D$, we hypothesize that $\hat{\mathbf{T}}_{\text{LP}}$ might serve as a good, analytically tractable, sub-optimal solution to (17). One important difference however is that unlike $\hat{\mathbf{T}}_{\text{FS}}$, $\hat{\mathbf{T}}_{\text{LP}}$ is independent of the switch position set \mathcal{S} , and therefore may have poor performance for some \mathcal{S} . To adapt $\hat{\mathbf{T}}_{\text{LP}}$ to a particular \mathcal{S} , we explore a greedy, column-permuting algorithm that increases $f_{\text{FS}}(\cdot)$, as depicted in Algorithm 1. The performance of this permuted matrix $\hat{\mathbf{T}}_{\text{Alg1}}$ may further be

⁶Note that if we use chordal distance metric [28] instead of Fubini-Study distance in $f_{\text{FS}}(\cdot)$, maximizing $f_{\text{FS}}(\cdot)$ *exactly* minimizes the largest cross-covariance term. However results suggest no significant gains are obtained by using this alternate distance metric and hence we restrict only to Fubini-Study distance.

⁷A semi-unitary matrix achieves the upper bound of $\min_{i \neq j} d_{\text{FS}}(\mathbf{Q}_i, \mathbf{Q}_j) = \min_{i \neq j} d_{\text{FS}}([\hat{\mathbf{T}}]_{c\{i\}}, [\hat{\mathbf{T}}]_{c\{j\}}) = \pi/2$.

improved via a numerical gradient ascent of $f_{\text{FS}}(\hat{\mathbf{T}})$, as depicted in Algorithm 2. Note that $\hat{\mathbf{T}}_{\text{LP}} \xrightarrow{\text{Algo1}} \hat{\mathbf{T}}_{\text{Alg1}} \xrightarrow{\text{Algo2}} \hat{\mathbf{T}}_{\text{Alg2}}$, where:

$$f_{\text{FS}}(\hat{\mathbf{T}}_{\text{LP}}) \leq f_{\text{FS}}(\hat{\mathbf{T}}_{\text{Alg1}}) \leq f_{\text{FS}}(\hat{\mathbf{T}}_{\text{Alg2}}) \leq f_{\text{FS}}(\hat{\mathbf{T}}_{\text{FS}}).$$

The complexities of Algorithms 1 and 2 are both $O(DL|\mathcal{S}|^2)$ per iteration, which can be

Algorithm 1: Greedy column permutation algorithm

```

1: Inputs:  $D, L, \mathcal{S}$ 
2: Initialize  $\hat{\mathbf{T}}$  {As obtained by line-packing [23]}
3: for  $\ell = 1$  to  $L$  do
4:   for  $j = 1$  to  $L$  do
5:      $\hat{\mathbf{T}}_{\text{Alg1}}(j) = \hat{\mathbf{T}}$ 
6:      $[\hat{\mathbf{T}}_{\text{Alg1}}(j)]_{c\{\ell\}} = [\hat{\mathbf{T}}]_{c\{j\}}$  and  $[\hat{\mathbf{T}}_{\text{Alg1}}(j)]_{c\{j\}} = [\hat{\mathbf{T}}]_{c\{\ell\}}$  {Swap columns  $\ell$  and  $j$ }
7:   end for
8:   Find  $j^*$  such that  $f_{\text{FS}}(\hat{\mathbf{T}}_{\text{Alg1}}(j^*))$  is largest
9:   if  $f_{\text{FS}}(\hat{\mathbf{T}}_{\text{Alg1}}(j^*)) > f_{\text{FS}}(\hat{\mathbf{T}})$  then
10:     $\hat{\mathbf{T}} = \hat{\mathbf{T}}_{\text{Alg1}}(j^*)$ 
11:   end if
12: end for
13: Repeat above process several times
14: return  $\hat{\mathbf{T}}$ 

```

substantial when $|\mathcal{S}|$ and/or L is large.

VII. REDUCING THE HARDWARE AND COMPUTATIONAL COMPLEXITY

A significant amount of analogue hardware may be required to implement the beamforming matrix and the switch bank of HBwS, especially for large values of D and L . In fact, a large $|\mathcal{S}|$ adds not only to the hardware cost but may also increase the computational complexity of picking the best selection matrix for each channel realization. In this section we shall discuss methods to reduce these hardware and computational costs.

A. Reducing hardware cost of the beamforming matrix

In general, we need a variable gain phase-shifter for each element of the $N \times L$ analogue beamforming matrix, thereby, needing NL components. This leads to a large implementation cost,

Algorithm 2: Gradient ascent algorithm for RD-beamformer design

```

1: Inputs:  $D, L, \mathcal{S}$ 
2: Initialize  $\hat{\mathbf{T}}, \gamma, \Delta T$ 
3:  $\hat{\mathbf{T}}_{\text{new}} = \hat{\mathbf{T}}$ 
4: while  $f_{\text{FS}}(\hat{\mathbf{T}}_{\text{new}}) \geq f_{\text{FS}}(\hat{\mathbf{T}})$  do
5:    $\hat{\mathbf{T}} = \hat{\mathbf{T}}_{\text{new}}$ 
6:   for  $i = 1$  to  $D$  do
7:     for  $j = 1$  to  $L$  do
8:        $\hat{\mathbf{T}}_{\Delta} = \hat{\mathbf{T}}$ 
9:        $[\hat{\mathbf{T}}_{\Delta}]_{ij} = [\hat{\mathbf{T}}]_{ij} + \Delta T$ 
10:       $\mathbf{F}_{ij} = \frac{f_{\text{FS}}(\hat{\mathbf{T}}_{\Delta}) - f_{\text{FS}}(\hat{\mathbf{T}})}{\Delta T}$  {Computing the gradient of objective function}
11:     end for
12:   end for
13:   for  $j = 1$  to  $L$  do
14:      $[\hat{\mathbf{F}}]_{c\{j\}} = [\mathbf{F}]_{c\{j\}} - [\hat{\mathbf{T}}]_{c\{j\}} [\hat{\mathbf{T}}]_{c\{j\}}^{\dagger} [\mathbf{F}]_{c\{j\}}$  {Ensuring unit norm columns}
15:   end for
16:    $\hat{\mathbf{T}}_{\text{new}} = \hat{\mathbf{T}} + \gamma \hat{\mathbf{F}}$ 
17:   for  $i = 1$  to  $D$  do
18:      $[\hat{\mathbf{T}}_{\text{new}}]_{c\{i\}} = [\hat{\mathbf{T}}_{\text{new}}]_{c\{i\}} / \left| [\hat{\mathbf{T}}_{\text{new}}]_{c\{i\}} \right|$  {Normalizing columns of  $\hat{\mathbf{T}}_{\text{new}}$ }
19:   end for
20: end while
21: return  $\hat{\mathbf{T}}$ 

```

especially when $L > D$. However, pre-assigning a fixed value \hat{D} to D , may allow significant savings when $L > D$, as detailed below. Firstly, by breaking the beamforming matrix into two components: $\mathbf{T} = \mathbf{T}_{\text{var}} \hat{\mathbf{T}}_{\text{fix}}$, where $\mathbf{T}_{\text{var}} = \mathbf{E}_{\text{tx}}^{\hat{D}} [\hat{\mathbf{T}}]_{c\{1:\hat{D}\}}$ and $\hat{\mathbf{T}}_{\text{fix}} = \left[\mathbb{I}_{\hat{D}} \quad [\hat{\mathbf{T}}]_{c\{1:\hat{D}\}}^{-1} [\hat{\mathbf{T}}]_{c\{(\hat{D}+1):L\}} \right]$ (as shown in Fig. 3), the number of required variable gain phase-shifters can be reduced from NL to $\hat{D}(N + L - \hat{D})$, which can be significant when $N \gg \hat{D}$. Here $\mathbf{E}_{\text{tx}}^{\hat{D}}$ is the $N \times \hat{D}$ sub-matrix of the eigen-vector matrix of \mathbf{R}_{tx} , corresponding to the largest \hat{D} eigenvalues. Secondly, since design of the RD-beamformer $\hat{\mathbf{T}}$ is independent of aCSI given D (see (7)), $\hat{\mathbf{T}}_{\text{fix}}$ can be pre-designed and its $\hat{D}(L - \hat{D})$ components can be implemented using a fixed phase-shifter array. The performance of this design when $D \neq \hat{D}$ is studied in section VIII. Further reduction in the hardware complexity can be obtained by using unit gain, discrete phase-shifter components for the beamformer [7], [8], [11]. The use and impact of such components is beyond the scope of this paper.

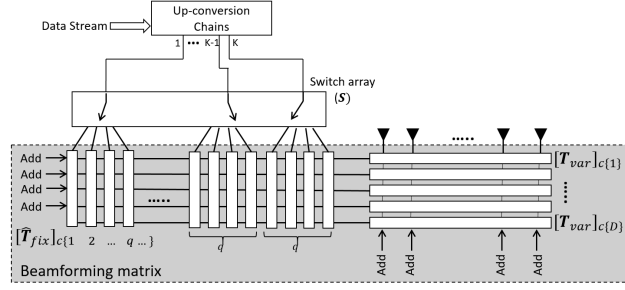


Fig. 3. Block diagram of a reduced complexity Hybrid Beamforming system with Selection

B. Restricting the size of the switch position set

In this subsection, we restrict the size of the switch position set \mathcal{S} . The size restriction not only reduces the hardware cost of implementing the switch bank, but also reduces the computational effort of picking the best selection matrix for a channel realization. In fact, since the \mathbf{Q}_i 's are coupled, some selection matrices may contribute little to the overall system performance.

Let us define for each selection matrix \mathbf{S}_i a corresponding set $\mathcal{B}_i \subset \{1, \dots, L\}$ such that $k \in \mathcal{B}_i$ iff $[\mathbf{S}_i]_{c\{m\}} = [\mathbb{I}_L]_{c\{k\}}$ for some $1 \leq m \leq K$. It can then be shown that $\mathbf{Q}_j^\dagger \mathbf{Q}_i \mathbf{Q}_i^\dagger \mathbf{Q}_j$ has $|\mathcal{B}_i \cap \mathcal{B}_j|$ unity eigenvalues (see appendix D). Therefore, we have:

$$\left[\lambda_K^\downarrow \{ \mathbf{Q}_j^\dagger \mathbf{Q}_i \mathbf{Q}_i^\dagger \mathbf{Q}_j \} \right]^{K-|\mathcal{B}_i \cap \mathcal{B}_j|} \leq |\mathbf{Q}_j^\dagger \mathbf{Q}_i \mathbf{Q}_i^\dagger \mathbf{Q}_j| \leq \left[\lambda_{|\mathcal{B}_i \cap \mathcal{B}_j|+1}^\downarrow \{ \mathbf{Q}_j^\dagger \mathbf{Q}_i \mathbf{Q}_i^\dagger \mathbf{Q}_j \} \right]^{K-|\mathcal{B}_i \cap \mathcal{B}_j|} \quad (21)$$

where $\lambda_k^\downarrow(\mathbf{A})$ represents the k -th largest eigenvalue of a matrix \mathbf{A} . From (21) and (10), a good way of increasing $C_{LB}^D(\hat{\mathbf{T}})$ in (12a) is to reduce $|\mathcal{B}_i \cap \mathcal{B}_j|$ for $i \neq j$. However, $|\mathcal{S}|$ should also be kept as large as possible to minimize the performance loss. In other words, we wish to find the largest family of subsets $\tilde{\mathcal{B}}$ such that:⁸

$$\tilde{\mathcal{B}} = \{ \mathcal{B}_1, \dots, \mathcal{B}_{|\tilde{\mathcal{B}}|} \mid \mathcal{B}_i \subseteq \{1, \dots, L\}, |\mathcal{B}_i| = K \text{ and } |\mathcal{B}_i \cap \mathcal{B}_j| \leq \kappa \ \forall i \neq j \}$$

Finding the largest such family is an open, but well studied, problem in the field of extremal combinatorics. Based on some of these results, we have the following theorem:

⁸ \mathcal{S} is the set of feasible selection matrices $\{\mathbf{S}_1, \dots, \mathbf{S}_{|\mathcal{S}|}\}$, and $\tilde{\mathcal{B}}$ is the corresponding set of subsets of column indices of \mathbf{T} .

Theorem VII.1 (K -uniform, $\{0 : \kappa\}$ -intersecting subsets). *For a given set of size L , the size of the largest set of subsets $\tilde{\mathcal{B}}$ such that each subset has cardinality K and no two subsets have more than κ elements in common is given by:*

$$\left[\frac{L}{2K} \right]^{\kappa+1} \leq q^{\kappa+1} \leq |\tilde{\mathcal{B}}| \leq \frac{^L C_{\kappa+1}}{^K C_{\kappa+1}} \quad \text{if, } L \geq 2K^2 \quad (22)$$

where q is the largest prime number such that $q \leq L/K$.

Proof. The upper bound is derived in [39] and an algorithm that achieves the lower bound was proposed in [40, Theorem 4.11], which is reproduced below for convenience. Let q be the largest prime number such that $q \leq L/K$. If $q \geq K$, a construction of a family of $q^{\kappa+1}$ subsets with the required, bounded overlap is given by Algorithm 3. Now from Bertrand's postulate [41], [42],

Algorithm 3: Frankl-Babai Construction [40]

```

1: for  $i = 1$  to  $q^{\kappa+1}$  do
2:    $\mathcal{B}_i = \emptyset$ 
3:   for  $j = 0$  to  $\kappa$  do
4:      $a_j = \text{mod}(i \mid q^j, q)$   {Here  $\mid$  implies integer division}
5:   end for
6:    $f(x) \triangleq \sum_{j=0}^{\kappa} a_j x^j$ 
7:   for  $k = 0$  to  $K - 1$  do
8:      $\mathcal{B}_i = \mathcal{B}_i \cup \{kq + \text{mod}(f(k), q) + 1\}$ 
9:   end for
10:  end for

```

there always exists a prime number q between $L/(2K)$ and L/K i.e., $q \geq L/(2K)$. Therefore a sufficient condition for Algorithm 3 is: $L/(2K) \geq K$. This concludes the theorem. \square

For $\tilde{\mathcal{B}}$ designed by Algorithm 3, each subset \mathcal{B}_i picks exactly one element in the interval $[kq, (k+1)q]$ for $k = 0, \dots, K-1$. Therefore the corresponding switch position set $\mathcal{S}_{\text{Alg3}(\kappa)} = \{\mathbf{S}_1, \dots, \mathbf{S}_{|\mathcal{S}_{\text{Alg3}(\kappa)}|}\}$ can be implemented by equipping each of the K up-conversion chains with a 1-to- q switch as depicted in Fig. 3. This leads to a significant saving in hardware cost as opposed a system with all possible selections, which requires a 1-to- $(L-1)$ switch for each up-conversion chain. Note that this reduced complexity structure is analogous to the design in [43] for conventional hybrid beamforming.

VIII. SIMULATION RESULTS

For simulations we consider a multi-user MIMO system with a multi-antenna TX implementing HBwS ($N = 100$) and one user group, having a common TX correlation matrix. The transmit correlation matrix has a dominant sub-space of dimension D with isotropic scattering within it i.e., $\Lambda_{\text{tx}}^D = \frac{N}{D} \mathbb{I}_D$. We consider a switch bank where each up-conversion chain has an exclusive set of input ports to connect to. Unless otherwise stated, we assume that all the switch positions possible with this architecture are allowed i.e.,:

$$\mathcal{S}_{\text{all}} = \left\{ [\mathbb{I}_L]_{c\{\ell_1, \dots, \ell_K\}} \left| (k-1) \left\lfloor \frac{L}{K} \right\rfloor < \ell_k \leq k \left\lfloor \frac{L}{K} \right\rfloor, k \in \{1, \dots, K\} \right. \right\}$$

Note that for the given channel model, the system capacity is independent of \mathbf{T} , given the RD-beamformer $\hat{\mathbf{T}}$. Therefore, without loss of generality, we quantify the system performance by $C^{\mathcal{D}}(\hat{\mathbf{T}})$ (see (8)). Since $C^{\mathcal{D}}(\hat{\mathbf{T}})$ is not known in closed form, throughout this section we use Monte-Carlo simulations to obtain its sample-mean estimate. A brute-force search is performed among \mathcal{S} to pick the best \mathbf{S} for each channel realization. The design of low-complexity algorithms for selecting \mathbf{S} is beyond the scope of this paper (see [21], [22] and references therein). Note that the performance of HBaCSI and HBiCSI can be obtained by replacing $\mathcal{S} = \{\mathbb{I}_K\}$ (no selection), $\hat{\mathbf{T}}_{\text{HBaCSI}} = [\mathbb{I}_D]_{c\{1:K\}}$ and $\hat{\mathbf{T}}_{\text{HBiCSI}} = [\mathbf{E}_{\text{ICSI}}^D]_{c\{1:K\}}$ in (8), where $\mathbf{E}_{\text{ICSI}}^D$ is the $D \times D$ eigen-vector matrix of $[\mathbf{E}_{\text{tx}}^D]^{\dagger} \tilde{\mathbf{H}}^{\dagger} \tilde{\mathbf{H}} \mathbf{E}_{\text{tx}}^D$.

A. Influence of number of input ports (L)

A comparison of the system sum capacity with HBwS as a function of number of input ports (L) is studied in Fig. 4. Here we plot the performance of both $\hat{\mathbf{T}}_{\text{Alg2}}$ and the line-packed RD-beamforming $\hat{\mathbf{T}}_{\text{LP}}$. We observe that with $L \approx D$ input ports, HBwS outperforms HBaCSI by approximately half the capacity gap between HBiCSI and HBaCSI. We also observe that there is a diminishing increase in performance as we increase the number of ports L . This suggests that, for a good trade-off between hardware cost and performance, L should be of the order of D i.e., $L \approx D$. Note however that D might not be known apriori and therefore L is a design choice for implementation. Results also suggest that for $\mathcal{S} = \mathcal{S}_{\text{all}}$, $\hat{\mathbf{T}}_{\text{LP}}$ and $\hat{\mathbf{T}}_{\text{Alg2}}$ have almost identical performance.

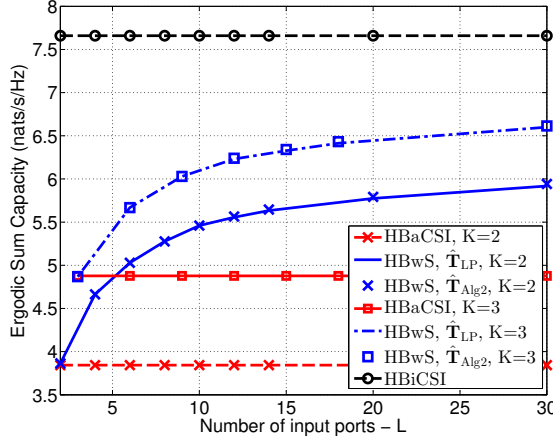


Fig. 4. Comparison of sum capacities $C^D(\hat{T}_{Alg2})$ and $C^D(\hat{T}_{LP})$, as a function of number of input ports L ($N = 100, D = 10, M = 2, \rho = 1, \mathcal{S} = \mathcal{S}_{all}$, \hat{T}_{LP} is generated using the MATLAB implementation of [37], $\Delta_{tx}^D = \frac{N}{D} \mathbb{I}_D$, $\mathbf{R}_{rx} = \mathbb{I}_M$)

B. Influence of restricted switch positions (\mathcal{S})

In this sub-section, we analyze the performance of HBwS under the restricted switch position sets $\mathcal{S}_{Alg3(\kappa)}$ from algorithm 3. Note that these restricted switch positions can be implemented using the switch bank architecture considered here. The sum-capacity $C^D(\hat{T}_{LP})$ with $\mathcal{S}_{Alg3(\kappa)}$ is compared to the average sum-capacity with a randomly chosen switch position set $\mathcal{S}_{rand(\kappa)}$, averaged over several realizations, in Fig. 5. The results support our claim that selection matrices with low overlap contribute more to system capacity than others. Results also show that while $|\mathcal{S}_{Alg3(\kappa)}|$ increases exponentially with κ , the increase in capacity is sub-linear, and therefore a small value of κ is sufficient to achieve good performance. Fig. 5 also compares the sum-rates $C^D(\hat{T}_{LP})$ and $C^D(\hat{T}_{Alg2})$ for $\mathcal{S} = \mathcal{S}_{Alg3(\kappa)}$, as a function of κ . The results suggest that even for these reduced complexity switch position sets, the line-packing solution \hat{T}_{LP} is almost as good as \hat{T}_{Alg2} . A similar trend has also been observed for several other switch position sets, not discussed in this paper for brevity. This suggests that the design \hat{T}_{LP} cannot be improved upon via conventional approaches such as algorithms 1 & 2. The good performance of \hat{T}_{LP} is due to the fact that when L is of the order of D , the semi-unitary matrices $\{\mathbf{Q}_i | 1 \leq i \leq |\mathcal{S}|\}$ are near orthogonal, and hence near optimal for (17) (see footnote 7). Henceforth, we shall avoid the use of the computationally intensive algorithms 1 & 2, and only restrict to use of \hat{T}_{LP} to study performance of HBwS.

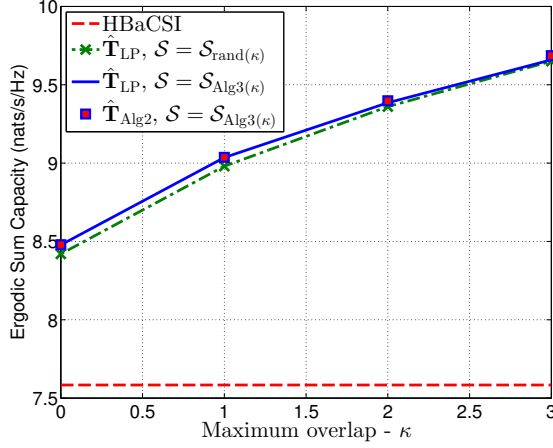


Fig. 5. Comparison of $C^D(\hat{\mathbf{T}}_{LP})$ with $\mathcal{S} = \mathcal{S}_{Alg3(\kappa)}$ to the average sum-capacity $E\{C^D(\hat{\mathbf{T}}_{LP})\}$ with $\mathcal{S} = \mathcal{S}_{rand(\kappa)}$, averaged over several realizations of $\mathcal{S}_{rand(\kappa)}$, as a function of maximum overlap κ . Here, $\mathcal{S}_{rand(\kappa)}$ is a randomly picked subset of \mathcal{S}_{all} such that $|\mathcal{S}_{rand(\kappa)}| = |\mathcal{S}_{Alg3(\kappa)}|$. For $\mathcal{S} = \mathcal{S}_{Alg3(\kappa)}$, we also plot $C^D(\hat{\mathbf{T}}_{Alg2})$. ($N = 100, D = 10, L = 20, K = M = 4, \rho = 1, \hat{\mathbf{T}}_{LP}$ is from MATLAB implementation of [37], $\kappa = \max_{i \neq j} |\mathcal{B}_i \cap \mathcal{B}_j|$ where $\hat{\mathcal{B}}$ is designed by algorithm 3, $\mathbf{A}_{tx}^D = \frac{N}{D} \mathbb{I}_D, \mathbf{R}_{rx} = \mathbb{I}_M$)

C. Influence of number of users (M_1)

We next consider the case where the system has a user group of M_1 single antenna users i.e., $M_2 = 1$. The sum capacity of HBwS (normalized by sum capacity of HBiCSI) for varying number of users is studied in Fig. 6. Apart from $C^D(\hat{\mathbf{T}}_{LP})$, which can be achieved via Dirty Paper Coding (DPC) [26], we also plot the normalized sum-rate for Zero-forcing (ZF) precoding with equal power allocation and random user scheduling⁹. Note that unlike with DPC, ZF precoding requires user scheduling to achieve good performance, and its sum rate with equal power allocation can be quantified as:

$$C_{ZF}(\mathbf{T}) = \mathbb{E}_{\tilde{\mathbf{H}}} \left\{ \max_{1 \leq i \leq |\mathcal{S}|} \left[|\mathcal{M}_{\text{sched}}(\tilde{\mathbf{H}})| \log \left(1 + \frac{\rho}{\text{Tr}\{(\tilde{\mathbf{H}}_{\text{sched}} \mathbf{T} \mathbf{S}_i \mathbf{G}_i \mathbf{G}_i^\dagger \mathbf{S}_i^\dagger \mathbf{T}^\dagger \tilde{\mathbf{H}}_{\text{sched}}^\dagger)^{-1}\}} \right) \right] \right\} \quad (23)$$

where $\tilde{\mathbf{H}}_{\text{sched}}$ is a sub-matrix of $\tilde{\mathbf{H}}$ (see (4)) corresponding to the set of scheduled users $\mathcal{M}_{\text{sched}}(\tilde{\mathbf{H}})$. We observe that the slope of the $C^D(\hat{\mathbf{T}}_{LP})$ curves, and hence fractional performance gain, increases with M . This suggests that the additional beam choices with HBwS may help improve user separability. Further, HBwS helps reduce the capacity gap between the linear precoding

⁹Sophisticated user scheduling algorithms such as [44] cannot be directly extended to HBwS due to the presence of switching.

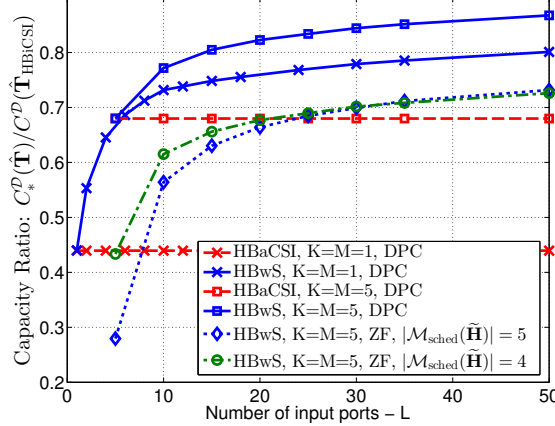


Fig. 6. Ergodic sum rate (normalized by the mean sum-rate of HBiCSI) versus L for varying number of users. For ZF precoding, $|\mathcal{M}_{\text{sched}}(\tilde{\mathbf{H}})|$ users, out of the M users, are randomly scheduled in each time slot. ($N = 100, D = 10, M_2 = 1, \rho = 1, \mathcal{S} = \mathcal{S}_{\text{all}}, \hat{\mathbf{T}}_{\text{LP}}$ is from [37], $\mathbf{\Lambda}_{\text{tx}}^D = \frac{N}{D} \mathbb{I}_D$, $\mathbf{R}_{\text{rx}} = \mathbb{I}_M$)

scheme - ZF, and the capacity optimal, non-linear precoding scheme - DPC, without requiring sophisticated user scheduling.

D. Influence of the dimension of dominant sub-space (D)

As elaborated in Section VII-A, pre-fixing the value of D to \hat{D} allows significant savings in the hardware implementation cost of HBwS. Therefore, it is important to study the sensitivity of the system performance to a mismatch in D . In Fig. 7, the performance of the RD-beamformers $\hat{\mathbf{T}}_{\text{LP}}(\hat{D})$ and $\hat{\mathbf{T}}_{\text{LP}}(D)$, designed for an estimated dimension of \hat{D} & D , respectively, is studied as a function of the actual channel dimension D . Results suggest that $C^D(\hat{\mathbf{T}}_{\text{LP}}(D))$ saturates beyond $D \geq K + 8$. Furthermore, the $C^D(\hat{\mathbf{T}}_{\text{LP}}(\hat{D}))$ degrades quickly when $D < \hat{D}$. Therefore, assuming D is sufficiently large, the reduced complexity beamformer in Section VII-A should be designed using a conservative estimate of $\hat{D} = K + 8$.

IX. ANISOTROPIC CHANNELS

In this section, we extend our beamformer design to anisotropic channels with $\mathbf{\Lambda}_{\text{tx}}^D \neq \frac{N}{D} \mathbb{I}_D$. Without loss of generality, we assume that the eigenvalues in $\mathbf{\Lambda}_{\text{tx}}^D$ are arranged in descending

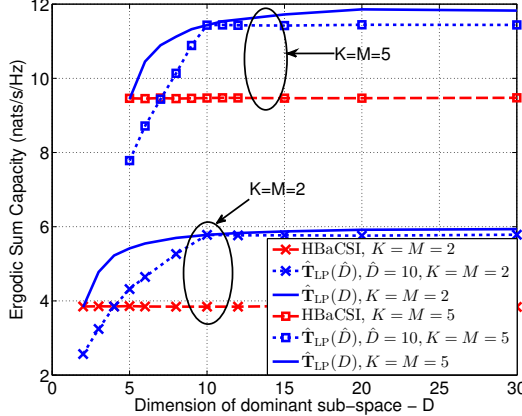


Fig. 7. Comparison of sum capacities $C^D(\hat{\mathbf{T}}_{\text{LP}}(\hat{D}))$ and $C^D(\hat{\mathbf{T}}_{\text{LP}}(D))$ as a function of D . Here $\hat{\mathbf{T}}_{\text{LP}}(A)$ represents the line-packed beamformer, designed for a dominant subspace dimension of A ($N = 100, \hat{D} = 10, \rho = D/10, \mathcal{S} = \mathcal{S}_{\text{all}}, \hat{\mathbf{T}}_{\text{LP}}$ is from the MATLAB implementation of [37], $\mathbf{\Lambda}_{\text{tx}}^D = \frac{N}{D} \mathbb{I}_D, \mathbf{R}_{\text{tx}} = \mathbb{I}_M$)

order of magnitude. Similar to the approach used in [30], [32], [45], we employ the companding trick to adapt the beamforming matrix to $\mathbf{\Lambda}_{\text{tx}}^D$, as:

$$\mathbf{T}_{\text{ani}} = \mathbf{E}_{\text{tx}}^D [\mathbf{\Lambda}_{\text{tx}}^D]^\xi \hat{\mathbf{T}}_{\text{LP}} \quad (24)$$

where $\hat{\mathbf{T}}_{\text{LP}}$ is the $D \times L$ line-packed RD-beamformer and ξ is the skewing parameter. Intuitively, (24) skews the columns of \mathbf{T}_{ani} , and therefore also the precoding beams $\mathbf{T}_{\text{ani}} \mathbf{S}_i \mathbf{G}_i$, to be more densely packed near the eigen-vectors corresponding to the larger eigenvalues of \mathbf{R}_{tx} . For $L > D$, this skewed beamformer can still be implemented using the two stage design in Sec VII-A by using $\mathbf{T}_{\text{var}} = \mathbf{E}_{\text{tx}}^{\hat{D}} [\mathbf{\Lambda}_{\text{tx}}^{\hat{D}}]^\xi [\hat{\mathbf{T}}_{\text{LP}}]_{c\{1:\hat{D}\}}$. In the current work we shall restrict to the case of $\xi = 1$ for brevity.¹⁰ It is worth mentioning that for $L \leq D$, not all line-packed matrices $\hat{\mathbf{T}}_{\text{LP}}$ yield good performance after skewing by (24). Therefore for $L \leq D$, we suggest the use of $\hat{\mathbf{T}}_{\text{LP}} = \left[\begin{array}{cc} \mathbf{W} & \mathbb{O}_{(D-L) \times L} \end{array} \right]^\dagger$ in (24), where \mathbf{W} is the $L \times L$ DFT matrix, i.e., $[\mathbf{W}]_{a,b} = e^{\frac{j2\pi ab}{L}} / \sqrt{L}$.

For simulations, we assume the TX has a half wavelength ($\lambda/2$) spaced uniform planar array of dimension 40×10 . The TX transmits to a user-group of $M_1 = 3$ single antenna receivers

¹⁰A line-search for the optimal skewing parameter ξ^* may further improve performance [27].

that share the same transmit power angle spectrum (PAS), given by:

$$\text{PAS}(\theta, \phi) = \sum_{i=1}^3 \exp[-\eta|\theta - \bar{\theta}_i| - \eta|\phi - \bar{\phi}_i|] \Pi(\theta - \bar{\theta}_i, \phi - \bar{\phi}_i) \quad (25)$$

$$\text{where: } \Pi(\theta, \phi) = \begin{cases} 1 & \text{for } |\theta| \leq \pi/20, |\phi| \leq \pi/20 \\ 0 & \text{otherwise} \end{cases},$$

$\bar{\theta} = \left[\frac{-3\pi}{10}, 0, \frac{\pi}{5}\right]$, $\bar{\phi} = \left[\frac{6\pi}{10}, \frac{8\pi}{10}, \frac{7\pi}{10}\right]$, $\theta \in [-\pi/2, \pi/2]$ is the azimuth angle of departure, $\phi \in [0, \pi)$ is the elevation angle of departure and η is a factor that controls the anisotropy of the channel. The transmit correlation matrix is computed as:

$$[\mathbf{R}_{\text{tx}}]_{ab} = \frac{\int_{-\pi/2}^{\pi/2} \int_0^\pi \text{PAS}(\theta, \phi) e^{j\pi d_H(a,b) \sin(\phi) \cos(\theta) + j\pi d_V(a,b) \cos(\phi) \sin(\phi)} d\phi d\theta}{\int_{-\pi/2}^{\pi/2} \int_0^\pi \text{PAS}(\theta, \phi) \sin(\phi) d\phi d\theta}$$

where $\lambda d_H(a, b)/2, \lambda d_V(a, b)/2$ are the horizontal and vertical separation distances between element a and b , respectively. It can be readily verified (using simulations) that for the PAS in (25) and $\forall \eta \geq 0$, \mathbf{R}_{tx} has at-most $D = 24$ dominant eigenvalues with negligible power outside. We denote the $N \times N$ eigen-vector matrix of \mathbf{R}_{tx} as \mathbf{E}_{tx} and its dominant $N \times D$ sub-matrix is denoted by \mathbf{E}_{tx}^D . For this channel, the performance of the skewed beamforming matrix \mathbf{T}_{ani} compared to $\mathbf{T}_{\text{LP}} \triangleq \mathbf{E}_{\text{tx}}^D \hat{\mathbf{T}}_{\text{LP}}$ is studied in Fig. 8 as a function of the channel anisotropy for the both cases of $L \leq D$ and $L > D$. For a comparison to existing designs, we also depict the performance of $\mathbf{T}_{\text{Sud}} \triangleq [\mathbf{E}_{\text{tx}}]_{c\{1:\min\{L, N\}\}}$, a generalization of the beamformer in [8]. Since \mathbf{T}_{Sud} is semi-unitary, i.e., a special case of \mathbf{T}_{LP} for $L \leq D$, it is not considered separately in section VIII. We observe from the results that the capacity gap between HBiCSI and HBaCSI reduces as the channel anisotropy increases. Also, unlike with \mathbf{T}_{LP} , the performance of \mathbf{T}_{ani} does not degrade with increasing anisotropy. Further, we observe that \mathbf{T}_{ani} outperforms both \mathbf{T}_{Sud} and HBaCSI, over the whole range of η for both $D \leq L$ and $D > L$. Therefore the designed beamformer is not only more generic (can be extended to the case of $L > N$) but also leads to better performance in comparison to existing designs.

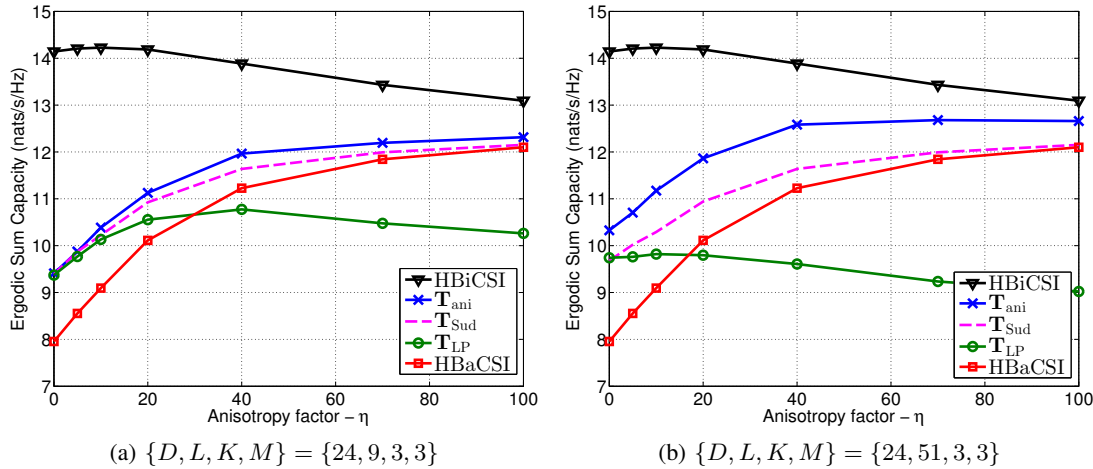


Fig. 8. Ergodic sum capacity for the skewed beamformer $\hat{\mathbf{T}}_{\text{ani}}$ as a function of channel anisotropy. (a) $\hat{\mathbf{T}}_{\text{LP}} = [\mathbf{W} \circledcirc_{(D-L) \times L}]^\dagger$, where \mathbf{W} is the $L \times L$ DFT matrix (b) $\hat{\mathbf{T}}_{\text{LP}}$ is from the line packing algorithm in [37] (simulation parameters: $N = 400$, $\mathcal{S} = \mathcal{S}_{\text{all}}$, $\mathbf{R}_{\text{rx}} = \mathbb{I}_M$ and $\rho = 1$).

X. CONCLUSIONS

In this work we propose a generic architecture for HBwS, as an attractive solution to reduce complexity and cost of massive MIMO systems. We show that a beamforming matrix that maximizes a lower bound to the system sum capacity is obtained by a coupled Grassmannian sub-space packing problem. We propose a good sub-optimal solution to the packing problem and explore algorithms to improve the design further for a given switch position set. We show that introducing a two stage beamforming matrix, having a fixed and an adaptive stage, can reduce the hardware cost of implementation significantly. We also show that switch positions with low overlap contribute more to system capacity than others, and provide an algorithm for finding a family of such important switch positions. Simulation results suggest that with $L \approx D$, HBwS can achieve gains comparable to half the capacity gap between HBaCSI and HBiCSI while requiring only aCSI to adapt the beamformer. We also conclude that for the explored switch position sets, the beamformer design $\hat{\mathbf{T}}_{LP}$ cannot be improved further via conventional approaches such as algorithms 1 & 2. Furthermore, for a good trade-off between performance and hardware cost, the number of input ports (L) should be of the order of D . However, larger values may be practical in a multi-user scenario, since a larger L can aid separation of multiple data streams. In particular, it helps make performance of linear ZF precoding comparable to

the non-linear and capacity optimal DPC without the need for sophisticated user scheduling algorithms. For implementing the two-stage beamformer, using a conservative estimate of D , of $\hat{D} = K + 8$, to design the fixed stage yields good performance. Results for anisotropic channels suggest that skewing the line-packed beamformer yields better performance in comparison to existing designs in the literature.

As is the case with other such diversity techniques [21], the performance gain of HBwS over HBaCSI decreases with frequency selective fading. This is because in the limit of a large transmission bandwidth, frequency diversity makes all the L selection ports equivalent. Hence, HBwS is more suited for small-to-medium bandwidth systems, where channels are at-most moderately frequency selective.

APPENDIX A

(*Proof of Theorem IV.1*). For any beamforming matrix \mathbf{T} we can write:

$$\mathbf{T} = \mathbf{E}_{tx} \mathbf{E}_{tx}^\dagger \mathbf{T} = \mathbf{E}_{tx}^D [\mathbf{E}_{tx}^D]^\dagger \mathbf{T} + \mathbf{E}_{tx}^{N-D} [\mathbf{E}_{tx}^{N-D}]^\dagger \mathbf{T} \quad (26)$$

where $\mathbf{E}_{tx}^D \triangleq [\mathbf{E}_{tx}]_{c\{1:D\}}$ and $\mathbf{E}_{tx}^{N-D} \triangleq [\mathbf{E}_{tx}]_{c\{D+1:N\}}$. Defining $\hat{\mathbf{T}} \triangleq [\mathbf{E}_{tx}^D]^\dagger \mathbf{T}$, for any user m , from (1) and (3) we have:

$$\begin{aligned} \mathbf{y}_m(\mathbf{S}_i) &= \sqrt{\rho} \mathbf{R}_{rx,m}^{1/2} \mathbf{H}_m [\Lambda_{tx}^D]^{1/2} [\mathbf{E}_{tx}^D]^\dagger \mathbf{T} \mathbf{S}_i \mathbf{x} + \mathbf{n}_m \\ &= \sqrt{\rho} \mathbf{R}_{rx,m}^{1/2} \mathbf{H}_m [\Lambda_{tx}^D]^{1/2} [\mathbf{E}_{tx}^D]^\dagger \mathbf{E}_{tx}^D \hat{\mathbf{T}} \mathbf{S}_i \mathbf{x} + \mathbf{n}_m \end{aligned} \quad (27)$$

where (27) follows from (26). Now, from the transmit power constraint in (2a) we have:

$$\begin{aligned} &\text{tr} \left\{ \mathbf{S}_i^\dagger \mathbf{T}^\dagger \mathbf{T} \mathbf{S}_i \mathbb{E}_x \{ \mathbf{x} \mathbf{x}^\dagger \} \right\} \leq 1 \\ \Rightarrow &\text{tr} \left\{ \mathbf{S}_i^\dagger \hat{\mathbf{T}}^\dagger [\mathbf{E}_{tx}^D]^\dagger \mathbf{E}_{tx}^D \hat{\mathbf{T}} \mathbf{S}_i \mathbb{E}_x \{ \mathbf{x} \mathbf{x}^\dagger \} \right\} + \text{tr} \left\{ \mathbf{S}_i^\dagger \mathbf{T}^\dagger \mathbf{E}_{tx}^{N-D} [\mathbf{E}_{tx}^{N-D}]^\dagger \mathbf{T} \mathbf{S}_i \mathbb{E}_x \{ \mathbf{x} \mathbf{x}^\dagger \} \right\} \leq 1 \end{aligned} \quad (28a)$$

$$\Rightarrow \text{tr} \left\{ \mathbf{E}_{tx}^D \hat{\mathbf{T}} \mathbf{S}_i \mathbb{E}_x \{ \mathbf{x} \mathbf{x}^\dagger \} \mathbf{S}_i^\dagger \hat{\mathbf{T}}^\dagger [\mathbf{E}_{tx}^D]^\dagger \right\} + \text{tr} \left\{ [\mathbf{E}_{tx}^{N-D}]^\dagger \mathbf{T} \mathbf{S}_i \mathbb{E}_x \{ \mathbf{x} \mathbf{x}^\dagger \} \mathbf{S}_i^\dagger \mathbf{T}^\dagger \mathbf{E}_{tx}^{N-D} \right\} \leq 1 \quad (28b)$$

$$\Rightarrow \text{tr} \left\{ \mathbf{E}_{tx}^D \hat{\mathbf{T}} \mathbf{S}_i \mathbb{E}_x \{ \mathbf{x} \mathbf{x}^\dagger \} \mathbf{S}_i^\dagger \hat{\mathbf{T}}^\dagger [\mathbf{E}_{tx}^D]^\dagger \right\} \leq 1 \quad (28c)$$

where (28a) follows from (26), (28b) follows from using the identity $\text{tr}\{\mathbf{AB}\} = \text{tr}\{\mathbf{BA}\}$ and (28c) follows from observing that both terms on left hand side are non-negative. From (28c) and

(27), for any $\mathbb{E}\{xx^\dagger\}$, if \mathbf{T} satisfies the power constraint then so does $\mathbf{E}_{\text{tx}}^D \hat{\mathbf{T}}$ and both $\mathbf{T}, \mathbf{E}_{\text{tx}}^D \hat{\mathbf{T}}$ yield the same instantaneous received signal $\mathbf{y}_m(\mathbf{S}_i)$. Therefore the optimization problem (6) can be reduced to $\mathbf{T}_{\text{opt}} = \mathbf{E}_{\text{tx}}^D \hat{\mathbf{T}}_{\text{opt}}$, where:

$$\hat{\mathbf{T}}_{\text{opt}} = \underset{\hat{\mathbf{T}} \in \mathbb{C}^{D \times L}}{\text{argmax}} \left\{ C(\mathbf{E}_{\text{tx}}^D \hat{\mathbf{T}}) \right\}$$

Note that $C(\mathbf{E}_{\text{tx}}^D \hat{\mathbf{T}})$ can be re-defined as in (8), where $\hat{\mathbf{G}}_i$ ortho-normalizes columns of $\mathbf{E}_{\text{tx}}^D \hat{\mathbf{T}} \mathbf{S}_i$ i.e., $\hat{\mathbf{G}}_i^\dagger \mathbf{S}_i^\dagger \hat{\mathbf{T}}^\dagger \hat{\mathbf{T}} \mathbf{S}_i \hat{\mathbf{G}}_i = \mathbb{I}_K$. \square

APPENDIX B

(*Proof of Theorem IV.2*). Let $\hat{\mathbf{T}} \in \mathbb{C}^{D \times L}$ be any $D \times L$ matrix. For each $\hat{\mathbf{T}} \mathbf{S}_i$ we have a corresponding $K \times K$ ortho-normalization matrix $\hat{\mathbf{G}}_i$. Now consider $\hat{\mathbf{T}}_\theta = \hat{\mathbf{T}} \Lambda_\theta$ where Λ_θ is any $L \times L$ non-singular complex diagonal matrix. For each selection matrix \mathbf{S}_i , by defining a corresponding matrix $\hat{\mathbf{G}}_{i\theta} \triangleq \mathbf{S}_i^\dagger \Lambda_\theta^{-1} \mathbf{S}_i \hat{\mathbf{G}}_i$, we have:

$$\hat{\mathbf{G}}_{i\theta}^\dagger \mathbf{S}_i^\dagger \hat{\mathbf{T}}_\theta^\dagger \hat{\mathbf{T}}_\theta \mathbf{S}_i \hat{\mathbf{G}}_{i\theta} = \hat{\mathbf{G}}_i^\dagger \mathbf{S}_i^\dagger [\Lambda_\theta^{-1}]^\dagger \mathbf{S}_i \mathbf{S}_i^\dagger \Lambda_\theta^\dagger \hat{\mathbf{T}}^\dagger \hat{\mathbf{T}} \Lambda_\theta \mathbf{S}_i \mathbf{S}_i^\dagger \Lambda_\theta^{-1} \mathbf{S}_i \hat{\mathbf{G}}_i \quad (29a)$$

$$= \hat{\mathbf{G}}_i^\dagger \mathbf{S}_i^\dagger \mathbf{S}_i \mathbf{S}_i^\dagger \hat{\mathbf{T}}^\dagger \hat{\mathbf{T}} \mathbf{S}_i \mathbf{S}_i^\dagger \mathbf{S}_i \hat{\mathbf{G}}_i \quad (29b)$$

$$= \hat{\mathbf{G}}_i^\dagger \mathbf{S}_i^\dagger \hat{\mathbf{T}}^\dagger \hat{\mathbf{T}} \mathbf{S}_i \hat{\mathbf{G}}_i \quad (29c)$$

$$= \mathbb{I}_K$$

where (29b) follows from the fact that $\mathbf{S}_i \mathbf{S}_i^\dagger$ is diagonal and hence commutes with Λ_θ and (29c) uses the fact that $\mathbf{S}_i^\dagger \mathbf{S}_i = \mathbb{I}_K$. This proves that $\hat{\mathbf{G}}_{i\theta}$ ortho-normalizes columns of $\hat{\mathbf{T}}_\theta \mathbf{S}_i$.

Using a similar sequence of steps it can be shown that $\hat{\mathbf{T}}_\theta \mathbf{S}_i \hat{\mathbf{G}}_{i\theta} \hat{\mathbf{G}}_{i\theta}^\dagger \mathbf{S}_i^\dagger \hat{\mathbf{T}}_\theta^\dagger = \hat{\mathbf{T}} \mathbf{S}_i \hat{\mathbf{G}}_i \hat{\mathbf{G}}_i^\dagger \mathbf{S}_i^\dagger \hat{\mathbf{T}}^\dagger$ and hence from (8), $C^D(\hat{\mathbf{T}}_\theta) = C^D(\hat{\mathbf{T}})$. This proves the theorem. \square

APPENDIX C

(*Proof of Lemma V.1*). Consider the decomposition $\mathbf{H} = \mathbf{U}_\mathbf{H} \Lambda_\mathbf{H} \mathbf{V}_\mathbf{H}^\dagger$, where $\mathbf{U}_\mathbf{H}$ is the $M \times M$ left singular-vector matrix, $\Lambda_\mathbf{H}$ is the $M \times M$ diagonal matrix containing the non-zero singular values, and $\mathbf{V}_\mathbf{H}$ is the $D \times M$ semi-unitary matrix containing the M right singular vectors

(corresponding to the non-zero singular values) for \mathbf{H} in (8).¹¹ Since \mathbf{H} has i.i.d. $\mathcal{CN}(0, 1)$ components, it is well known that $\mathbf{U}_{\mathbf{H}}\Lambda_{\mathbf{H}}$ and $\mathbf{V}_{\mathbf{H}}$ are independently distributed and further, $\mathbf{V}_{\mathbf{H}}$ is uniformly distributed over $\mathcal{U}(D, M)$ [28, Lemma 4]. Now, using the fact that $|\mathbb{I} + \mathbf{A}| \geq 1 + |\mathbf{A}|$ for any positive semi-definite matrix \mathbf{A} , we can lower bound $C^{\mathcal{D}}(\hat{\mathbf{T}})$ in (8), for $\Lambda_{\text{tx}}^D = \frac{N}{D}\mathbb{I}_D$, as:

$$C^{\mathcal{D}}(\hat{\mathbf{T}}) \geq \mathbb{E}_{\Lambda_{\mathbf{H}}}\mathbb{E}_{\mathbf{V}_{\mathbf{H}}} \left\{ \max_{1 \leq i \leq |S|} \log \left[1 + \alpha \left| \mathbf{V}_{\mathbf{H}}^{\dagger} \mathbf{Q}_i \mathbf{Q}_i^{\dagger} \mathbf{V}_{\mathbf{H}} \right| \right] \right\} \quad (30)$$

where $\alpha = \left(\frac{\rho N}{MD}\right)^M |\mathbf{R}_{\text{rx}}| |\Lambda_{\mathbf{H}}|^2$. The lower bound in (30) is tight in the high SNR regime i.e., when $\rho |\mathbf{R}_{\text{rx}}|^{1/M} N/M \gg 1$.

Consider a random $D \times K$ matrix \mathbf{V} , independent of \mathbf{H} and uniformly distributed over $\mathcal{U}(D, K)$. Since the uniform measure is invariant under unitary transformation, for any $D \times D$ unitary matrix \mathbf{U} , we have:

$$\mathbf{V} \stackrel{d}{=} \mathbf{U}\mathbf{V} \Rightarrow [\mathbf{V}]_{c\{1:M\}} \stackrel{d}{=} \mathbf{U}[\mathbf{V}]_{c\{1:M\}}$$

Since $[\mathbf{V}]_{c\{1:M\}}$ is a $D \times M$ semi-unitary matrix and is unitarily invariant, $[\mathbf{V}]_{c\{1:M\}}$ is uniformly distributed over $\mathcal{U}(D, M)$ and $\mathbf{V}_{\mathbf{H}} \stackrel{d}{=} [\mathbf{V}]_{c\{1:M\}}$. Now, from (30) we have:

$$C^{\mathcal{D}}(\hat{\mathbf{T}}) \geq \mathbb{E}_{\Lambda_{\mathbf{H}}}\mathbb{E}_{\mathbf{V}} \left\{ \max_{1 \leq i \leq |S|} \log \left[1 + \alpha \left| [\mathbf{V}]_{c\{1:M\}}^{\dagger} \mathbf{Q}_i \mathbf{Q}_i^{\dagger} [\mathbf{V}]_{c\{1:M\}} \right| \right] \right\} \quad (31)$$

Note that $[\mathbf{V}]_{c\{1:M\}}^{\dagger} \mathbf{Q}_i \mathbf{Q}_i^{\dagger} [\mathbf{V}]_{c\{1:M\}}$ is the $M \times M$ principal sub-matrix of $\mathbf{V}^{\dagger} \mathbf{Q}_i \mathbf{Q}_i^{\dagger} \mathbf{V}$. Therefore using the Cauchy's Interlacing Theorem [46, Corollary 3.1.5], we have $\forall 1 \leq i \leq M$:

$$1 \geq \lambda_i^{\downarrow} \{ [\mathbf{V}]_{c\{1:M\}}^{\dagger} \mathbf{Q}_i \mathbf{Q}_i^{\dagger} [\mathbf{V}]_{c\{1:M\}} \} \geq \lambda_{i+(K-M)}^{\downarrow} \{ \mathbf{V}^{\dagger} \mathbf{Q}_i \mathbf{Q}_i^{\dagger} \mathbf{V} \} \geq 0 \quad (32)$$

where, $\lambda_k^{\downarrow}\{\mathbf{A}\}$ represents the k -th largest eigenvalue of a square matrix \mathbf{A} and the unity upper bound comes from the fact that both \mathbf{V} and \mathbf{Q}_i are semi-unitary. Since the determinant is the product of eigenvalues, from (31) and (32), we arrive at (11). Note that $|\Lambda_{\mathbf{H}}|^2 = |\mathbf{H}\mathbf{H}^{\dagger}|$. \square

¹¹Note that this is slightly different from the usual approach of singular value decomposition.

APPENDIX D

Let us define for each selection matrix \mathbf{S}_i a corresponding set $\mathcal{B}_i \subset \{1, \dots, L\}$ such that $k \in \mathcal{B}_i$ iff $[\mathbf{S}_i]_{c\{m\}} = [\mathbb{I}_L]_{c\{k\}}$ for some $1 \leq m \leq K$. Then for any $\ell \in \mathcal{B}_i \cap \mathcal{B}_j$, we have $[\hat{\mathbf{T}}]_{c\{\ell\}} \in \text{column-space}\{\mathbf{Q}_i\} \cap \text{column-space}\{\mathbf{Q}_j\}$ i.e., there exists a $K \times 1$ vector \mathbf{t}_ℓ such that $\mathbf{Q}_j \mathbf{t}_\ell = [\hat{\mathbf{T}}]_{c\{\ell\}}$. Furthermore, since \mathbf{Q}_i 's are semi-unitary, we have for any $\ell \in \mathcal{B}_i \cap \mathcal{B}_j$:

$$\begin{aligned} \mathbf{Q}_i \mathbf{Q}_i^\dagger [\hat{\mathbf{T}}]_{c\{\ell\}} &= [\hat{\mathbf{T}}]_{c\{\ell\}} \\ \Rightarrow \mathbf{Q}_j^\dagger \mathbf{Q}_i \mathbf{Q}_i^\dagger \mathbf{Q}_j \mathbf{t}_\ell &= \mathbf{t}_\ell \end{aligned}$$

i.e., \mathbf{t}_ℓ is an eigen-vector of $\mathbf{Q}_j^\dagger \mathbf{Q}_i \mathbf{Q}_i^\dagger \mathbf{Q}_j$ with eigenvalue 1. If the vectors $\{[\hat{\mathbf{T}}]_{c\{\ell\}} | \ell \in \mathcal{B}_i \cap \mathcal{B}_j\}$ are linearly independent, then so are $\{\mathbf{t}_\ell | \ell \in \mathcal{B}_i \cap \mathcal{B}_j\}$. Therefore, $\mathbf{Q}_j^\dagger \mathbf{Q}_i \mathbf{Q}_i^\dagger \mathbf{Q}_j$ has $|\mathcal{B}_i \cap \mathcal{B}_j|$ unity eigenvalues.

REFERENCES

- [1] T. Marzetta, “Noncooperative Cellular Wireless with Unlimited Numbers of Base Station Antennas,” *IEEE Transactions on Wireless Communications*, vol. 9, pp. 3590–3600, November 2010.
- [2] F. Boccardi, R. Heath, A. Lozano, T. Marzetta, and P. Popovski, “Five disruptive technology directions for 5G,” *IEEE Communications Magazine*, vol. 52, pp. 74–80, February 2014.
- [3] K. I. Pedersen, P. E. Mogensen, and B. H. Fleury, “A stochastic model of the temporal and azimuthal dispersion seen at the base station in outdoor propagation environments,” *IEEE Transactions on Vehicular Technology*, vol. 49, pp. 437–447, Mar 2000.
- [4] M. Akdeniz, Y. Liu, M. Samimi, S. Sun, S. Rangan, T. Rappaport, and E. Erkip, “Millimeter wave channel modeling and cellular capacity evaluation,” *IEEE Journal on Selected Areas in Communications*, vol. 32, pp. 1164–1179, June 2014.
- [5] K. Haneda, J. Zhang, L. Tan, G. Liu, *et al.*, “5G 3GPP-like channel models for outdoor urban microcellular and macrocellular environments,” in *IEEE 83rd Vehicular Technology Conference (VTC Spring)*, pp. 1–7, 2016.
- [6] X. Zhang, A. Molisch, and S.-Y. Kung, “Phase-shift-based antenna selection for MIMO channels,” in *IEEE Global Telecommunications Conference (GLOBECOM '03)*, vol. 2, pp. 1089–1093 Vol.2, Dec 2003.
- [7] X. Zhang, A. Molisch, and S.-Y. Kung, “Variable-phase-shift-based RF-baseband codesign for MIMO antenna selection,” *IEEE Transactions on Signal Processing*, vol. 53, pp. 4091–4103, Nov 2005.
- [8] P. Sudarshan, N. Mehta, A. Molisch, and J. Zhang, “Channel statistics-based RF pre-processing with antenna selection,” *IEEE Transactions on Wireless Communications*, vol. 5, pp. 3501–3511, December 2006.
- [9] P. D. Karamalis, N. D. Skentos, and A. G. Kanatas, “Adaptive antenna subarray formation for MIMO systems,” *IEEE Transactions on Wireless Communications*, vol. 5, pp. 2977–2982, November 2006.

- [10] O. El Ayach, R. Heath, S. Abu-Surra, S. Rajagopal, and Z. Pi, “The capacity optimality of beam steering in large millimeter wave MIMO systems,” in *Signal Processing Advances in Wireless Communications (SPAWC), 2012 IEEE 13th International Workshop on*, pp. 100–104, June 2012.
- [11] A. Alkhateeb, O. El Ayach, G. Leus, and R. Heath, “Hybrid precoding for millimeter wave cellular systems with partial channel knowledge,” in *Information Theory and Applications Workshop (ITA)*, pp. 1–5, Feb 2013.
- [12] NTT Docomo, “Initial Performance Investigation of Hybrid Beamforming,” Tech. Rep. R1-167384, 3GPP, Gothenburg, Sweden, August 2016.
- [13] A. F. Molisch, V. V. Ratnam, S. Han, Z. Li, S. L. H. Nguyen, L. Li, and K. Haneda, “Hybrid beamforming for massive MIMO - A survey,” *CoRR*, vol. abs/1609.05078, 2016.
- [14] O. El Ayach, S. Rajagopal, S. Abu-Surra, Z. Pi, and R. Heath, “Spatially sparse precoding in millimeter wave MIMO systems,” *IEEE Transactions on Wireless Communications*, vol. 13, pp. 1499–1513, March 2014.
- [15] Z. Xu, S. Han, Z. Pan, and C.-L. I, “Alternating beamforming methods for hybrid analog and digital mimo transmission,” in *IEEE International Conference on Communications (ICC)*, pp. 1595–1600, June 2015.
- [16] A. Adhikary, J. Nam, J.-Y. Ahn, and G. Caire, “Joint spatial division and multiplexing – the large-scale array regime,” *IEEE Transactions on Information Theory*, vol. 59, pp. 6441–6463, Oct 2013.
- [17] 3GPP, “Technical Specification Group Radio Access Network; Study on 3D channel model for LTE (Release 12),” Tech. Rep. v12.2.0, 3rd Generation Partnership Project (3GPP), Valbonne, France, June 2015.
- [18] R. Méndez-Rial, C. Rusu, N. González-Prelcic, A. Alkhateeb, and R. W. Heath, “Hybrid MIMO architectures for millimeter wave communications: Phase shifters or switches?,” *IEEE Access*, vol. 4, pp. 247–267, 2016.
- [19] V. V. Ratnam, A. F. Molisch, N. Rabeah, F. Alawwad, and H. Behairy, “Diversity versus training overhead trade-off for low complexity switched transceivers,” in *IEEE Global Communications Conference (GLOBECOM)*, pp. 1–6, Dec 2016.
- [20] D. Gore and A. Paulraj, “MIMO antenna subset selection with space-time coding,” *IEEE Transactions on Signal Processing*, vol. 50, pp. 2580–2588, Oct 2002.
- [21] A. F. Molisch and M. Z. Win, “MIMO systems with antenna selection,” *IEEE Microwave Magazine*, vol. 5, pp. 46–56, Mar 2004.
- [22] S. Sanayei and A. Nosratinia, “Antenna selection in MIMO systems,” *IEEE Communications Magazine*, vol. 42, pp. 68–73, Oct 2004.
- [23] V. V. Ratnam, O. Y. Bursalioglu, H. Papadopoulos, and A. Molisch, “Preprocessor design for hybrid preprocessing with selection in massive MISO systems,” in *IEEE International Conference on Communications (ICC)*, (Paris, France), May 2017.
- [24] J. Kermoal, L. Schumacher, K. Pedersen, P. Mogensen, and F. Frederiksen, “A stochastic MIMO radio channel model with experimental validation,” *IEEE Journal on Selected Areas in Communications*, vol. 20, pp. 1211–1226, Aug 2002.
- [25] S. Vishwanath, N. Jindal, and A. Goldsmith, “Duality, achievable rates, and sum-rate capacity of Gaussian MIMO broadcast channels,” *IEEE Transactions on Information Theory*, vol. 49, pp. 2658–2668, Oct 2003.
- [26] G. Caire and S. Shamai, “On the achievable throughput of a multiantenna gaussian broadcast channel,” *IEEE Transactions on Information Theory*, vol. 49, pp. 1691–1706, July 2003.
- [27] V. V. Ratnam, A. F. Molisch, and H. C. Papadopoulos, “MIMO systems with restricted pre/post-coding – capacity analysis

based on coupled doubly correlated Wishart matrices," *IEEE Transactions on Wireless Communications*, vol. 15, pp. 8537–8550, Dec 2016.

[28] D. Love and R. Heath, "Limited feedback unitary precoding for spatial multiplexing systems," *IEEE Transactions on Information Theory*, vol. 51, pp. 2967–2976, Aug 2005.

[29] D. Love, R. Heath, V. Lau, D. Gesbert, B. Rao, and M. Andrews, "An overview of limited feedback in wireless communication systems," *IEEE Journal on Selected Areas in Communications*, vol. 26, pp. 1341–1365, October 2008.

[30] D. Love and R. Heath, "Grassmannian beamforming on correlated MIMO channels," in *IEEE Global Telecommunications Conference (GLOBECOM '04)*, vol. 1, pp. 106–110 Vol.1, Nov 2004.

[31] V. Raghavan, A. Sayeed, and V. Veeravalli, "Limited feedback precoder design for spatially correlated MIMO channels," in *41st Annual Conference on Information Sciences and Systems (CISS '07)*, pp. 113–118, March 2007.

[32] V. Raghavan and V. Veeravalli, "Ensemble properties of RVQ-based limited-feedback beamforming codebooks," *IEEE Transactions on Information Theory*, vol. 59, pp. 8224–8249, Dec 2013.

[33] D. Love, R. Heath, and T. Strohmer, "Grassmannian beamforming for multiple-input multiple-output wireless systems," *IEEE Transactions on Information Theory*, vol. 49, pp. 2735–2747, Oct 2003.

[34] N. R. Goodman, "The distribution of the determinant of a complex wishart distributed matrix," *Ann. Math. Statist.*, vol. 34, pp. 178–180, 03 1963.

[35] A. Barg and D. Y. Nogin, "Bounds on packings of spheres in the Grassmann manifold," *IEEE Transactions on Information Theory*, vol. 48, pp. 2450–2454, Sep 2002.

[36] R. A. Vitale, "Some comparisons for gaussian processes," *Proceedings of the American Mathematical Society*, vol. 128, no. 10, pp. 3043–3046, 2000.

[37] A. Medra and T. N. Davidson, "Flexible codebook design for limited feedback downlink systems via smooth optimization on the grassmannian manifold," in *IEEE 13th International Workshop on Signal Processing Advances in Wireless Communications (SPAWC)*, pp. 50–54, June 2012.

[38] I. S. Dhillon, R. W. Heath, T. Strohmer, and J. A. Tropp, "Constructing packings in Grassmannian manifolds via alternating projection," *Experiment. Math.*, vol. 17, no. 1, pp. 9–35, 2008.

[39] M. Deza, P. Erdos, and P. Frankl, "Intersection properties of systems of finite sets," *Proceedings of London Math. Society*, vol. 36, no. 3, pp. 369 – 384, 1978.

[40] L. Babai and P. Frankl, *Linear Algebra Methods in Combinatorics with Applications to Geometry and Computer Science*. Department of Computer Science, The University of Chicago, 1992.

[41] S. Ramanujan, "A proof of bertrand's postulate," *Journal of Indian Math. Society*, vol. 11, pp. 181 – 182, 1919. available at <http://www.imsc.res.in/~rao/ramanujan/CamUniCpapers/Cpaper24/> page1.html.

[42] J. Sondow and E. W. Weisstein, "Bertrand's postulate..," *From MathWorld—A Wolfram Web Resource*. available at <http://mathworld.wolfram.com/BertrandsPostulate.html>.

[43] Z. Xu, S. Han, Z. Pan, and C. L. I, "Alternating beamforming methods for hybrid analog and digital MIMO transmission," in *IEEE International Conference on Communications (ICC)*, pp. 1595–1600, June 2015.

[44] G. Dimic and N. D. Sidiropoulos, "On downlink beamforming with greedy user selection: performance analysis and a simple new algorithm," *IEEE Transactions on Signal Processing*, vol. 53, pp. 3857–3868, Oct 2005.

- [45] P. Xia and G. B. Giannakis, “Design and analysis of transmit-beamforming based on limited-rate feedback,” *IEEE Transactions on Signal Processing*, vol. 54, pp. 1853–1863, May 2006.
- [46] R. Bhatia, *Matrix Analysis (Graduate Texts in Mathematics)*. Springer New York, 1997.